Seasonal compound renewable energy droughts in the Unites States

Cameron Bracken[a], Nathalie Voisin[a,b], Youngjun Son[a], Sha Feng[a], Osten Anderson[a], Xiaodong Chen[a], He Li[a], Konstantinos Oikonomou[a]

[a] *Pacific Northwest National Laboratory, Richland, WA, USA*
[b] *University of Washington, Seattle, WA, USA*

Abstract

Variable renewable energy (VRE) droughts are periods of low renewable electricity production due to natural variability in the weather and climate. These compound renewable energy droughts occur when two or more (typically wind and solar) generation sources are in low availability conditions at the same time. Compound wind and solar droughts are most commonly studied at the hourly and daily timescale due to the short-term nature of energy markets and battery storage capacity. However the seasonal time scale allows for the examination of broader climate and hydrologic patterns that influence a broader renewable energy portfolio and inform the needs for long-duration energy storage. In this study, we use a newly developed dataset of coincident renewable generation to characterize seasonal compound VRE droughts which include wind, solar and hydropower at grid-relevant spatial scales across the contiguous United States. Along with the frequency, duration, magnitude, and spatial scale, we specifically examine these climate patterns with a composite climate analysis. Results for the historical period (1982-2019) indicate that seasonal compound VRE droughts can last up to 5 months and occur most frequently in the Fall. While not an established "climate stress" to consider in reliability studies yet, we demonstrate the impact of seasonal energy droughts on a resource adequacy study over the Western US interconnection using a nodal bulk power grid model. We further discuss how seasonal compound VREs can inform the sizing of long-duration energy storage and market incentives to manage short-term extreme events like heat waves and cold snaps while considering seasonal conditions.

Keywords:

1. Introduction

Variable renewable energy (VRE) droughts refer to naturally occurring periods of low energy availability from a resource such as wind, solar, and hydropower whose generation output is dependent on the weather or hydrologic cycle. VRE droughts have been shown to have highly regional properties that depend on both the local climatology and the specific makeup of the renewable generation and transmission infrastructure in a particular region [1, 2, 3, 4]. Compound VRE droughts refer to periods in which two or more generation sources are simultaneously experiencing drought conditions. Acute compound VRE events are necessarily more rare but can have much greater impacts to the grid in terms of increased costs, higher carbon emissions, or energy shortfalls [5, 6, 2].

Previous VRE drought studies [7, 2, 8, 3, 1, 9, 10, 11, 12, 13, 14, 15, 16, 17, 18, 4, 19] typically focus on short timescales of hours to days which are particularly relevant for grid stability [20] and energy storage [21]. Droughts which can occur on longer timescales of months to years are not commonly studied despite their implications for resource adequacy and at least higher green house gas emissions when renewable generation must be replaced [22, 23]. In this study we seek to examine energy droughts on the seasonal timescale, which has typically been the focus of resource adequacy studies [24, 25].

Most studies of VRE drought do not consider hydropower due to the different timescale compared to wind and solar and the relative complexity of extending the analyses with large scale hydrologic modeling, water uses and associated water management. Raynaud et al. [1] analyze wind, solar and hydropower droughts independently in Europe but they do not consider compound events. Francois et al. [26] assess the statistical properties of solar and hydropower droughts to reduce their compound occurrences in Northern Italy. However, these studies incorporate hydrologic representations that are confined to run-of-river hydropower with no seasonal reservoir storage management. Most et al. [27] examine compound wind, solar and hydropower droughts in Europe finding that appropriately managing reservoirs in winter is critical to mitigating and recovering from compound events. Woerman et al. [28] look at the complementarity of wind, solar and hydropower generation across Europe finding that droughts can be mitigated through a combination of transmission and storage at the continental scale. We note that even when water conditions might be low, hydropower operations are managed to provide a number of ancillary grid services such as operating reserves, voltage support, blackstart and load factoring which are particularly valuable alongside wind and solar generation [29]. Hydropower, encompassing both run-of-river and reservoir storage types, is therefore important to consider in compound VRE drought studies that focus on longer timescales. Pumped storage hydro is economically designed to address shorter term storage needs and is not considered in this study.

Previous studies have shown that large-scale atmospheric circulations and climate modes, such as weather regimes and teleconnection patterns like the North Atlantic Oscillation (NAO) and Pacific-North American (PNA), have predictability for seasonal renewable energy generation[30, 31, 32, 33, 34, 11, 35, 36, 14, 5, 15, 37]. For example, during the first quarter of 2015, the United States (U.S.) experienced a widespread and extended period of low surface wind speeds, which significantly impacted wind power generation. Some wind farms failed to generate enough income to cover their steady payments, causing the value of certain assets to decrease. [33] found this wind energy drought event was due to high sea surface temperatures in the western tropical Pacific Ocean associated with a strongly positive phase of the North Pacific Mode, which played a crucial role in establishing and maintaining persistent low wind events. [38] demonstrated that the dominant source of skillful subseasonal-to-seasonal prediction for wind energy resources over the contiguous United States (CONUS) mainly comes from year-to-year variations of El Niño-Southern Oscillation (ENSO) in the tropical Pacific, which alters large-scale wind and storm track patterns over the CONUS. There are several studies examining relationships between climate conditions and the availability of specific renewable energy resources, such as solar or wind. However, research focusing on the atmospheric drivers of compound energy droughts is rare. [5] analyzed the relationship between compound solar radiation and wind speed droughts with weather systems and climate modes and found that these droughts occur most frequently in winter, affecting at least five key energy-producing regions in Australia on 10% of days. The associated weather systems vary by season and drought type, but common features include widespread cloud cover and anticyclonic circulation patterns. Major climate modes are not strong predictors of grid-wide droughts, though regional variations exist that influence drought frequencies. In this study, we examine how large-scale circulations and climate modes contribute to seasonal compound VRE droughts over the CONUS. The mechanisms identified may be useful for developing forecasting models or seasonal energy drought outlooks.

The impacts of VRE drought are not realized until they occur during periods of high energy demand. One way to assess impacts to the energy system is to examine VRE droughts alongside energy demand which are known as VRE supply droughts or positive residual load (PRL) events [39, 4]. While this type of analysis can provide insights into potential regional energy shortfalls, it lacks detailed system information such the impacts on energy prices, transmission congestion and unserved energy, and carbon emissions. Such information is provided by a nodal production cost model (PCM), a detailed unit commitment and economic dispatch model. In this paper we develop a CONUS-wide assessment of compound seasonal wind–solar–hydropower droughts which we complement with a case study that integrates five separate compound VRE drought events into the a PCM. The goal of this case study is to demonstrate the value of considering compound seasonal VRE drought in resource adequacy studies. Section 2 discusses the data used and how seasonal compound VRE drought events were identified, Section 3 examines the historical properties, Section 4 looks at the spatial co-occurrence characteristics, Section 5 presents a composite climate analysis of the conditions that lead to compound VRE drought, Section 6 presents a case study that demonstrates how drought events can be incorporated into a power system model, and Section 7 is discussion.

2. Identification of Seasonal Compound VRE Droughts

Coincident and consistent plant-scale datasets for wind, solar [4], and hydropower [40] generation were analyzed to identify monthly energy drought events with 2020 infrastructure and historical weather conditions. Here, we briefly summarize the development of each dataset, as detailed descriptions are available in the cited literature. Historical meteorological data (1982-2019) from the Thermodynamic Global Warming (TGW) climate simulations [41] were utilized to estimate coincident energy generation from wind, solar, and hydropower renewable resources. In the TGW climate simulations, the Weather Research and Forecasting (WRF) model [42] was used to dynamically downscale the European Centre for Medium-Range Weather Forecast Version 5 Reanalysis (ERA5) [43].

Wind and solar generation was estimated for every utility scale wind and solar plant in the EIA 860 database [44]. Plant characteristics (turbine height, rotor diameter, solar panel type, etc.) were combined with the TGW meteorology data using NREL's reV model [45] to produce hourly plant-scale generation estimates. The solar radiation data was observed to have a high bias relative to observations in the National Solar Radiation Database (NSRDB)[46]. To account for this bias, the solar generation was bias corrected using NSRDB as a baseline. For full details please see [47].

Hydropower generation was estimated at individual facilities based on integrated hydrologic modeling to simulate runoff, a river routing-reservoir operations-water management model for regulated streamflow, and a hydropower model. The calculations of surface and subsurface runoff were performed using the Variable Infiltration Capacity (VIC) model [48, 49], which was calibrated at each $1/16^{\text{th}}$ degree grid cell using the daily runoff dataset from the Global Reach-level Flood Reanalysis (GRFR) ReachHydro product [50, 51]. The generated runoff was subsequently aggregated to $1/8^{\text{th}}$ degree grids and routed using the mosartwmpy model [52], a Python translation of the Model for Scale Adaptive River Transport with Water Management (MOSART-WM) [53, 54]. The mosartwmpy model simulates regulated streamflow influenced by water management components, including reservoir operations and water withdrawals. The data-driven approach [55] was implemented for reservoir operations with reasonable data coverage. Hydropower estimates are developed using the B1hydro model [40] which uses reservoir outflow, inflow, storage, and previous lagged power to estimate monthly power generation.

Seasonal compound VRE droughts are identified by first spatially aggregating all individual plants to the the Balancing Authority (BA) scale. BAs are entities in the U.S. where supply and demand must be balanced at all times and specifically need to use local resources to balance the local "must-take" wind and solar resources. The BA represents a grid-relevant scale at which to analyze VRE droughts. BA-scale wind, solar, and hydropower generation data are then temporally aggregated to the monthly timescale. The monthly timescale is used because it can represent droughts which last at least 1 month so they can represent seasonal drought events. Table 2 shows the considered BAs. In this study, a seasonal compound VRE drought is defined as any period of consecutive months for which the total generation from wind, solar and hydropower is below the 40th percentile for each generation type. This threshold was chosen to be representative of consistently low renewable generation that still represents a range of drought events across the contiguous U.S. Based on the threshold, the severity of compound VRE droughts is defined as the normalized energy deficit below the threshold [4].

BA	BA name	NERC* grid interconnect	Cluster	Hydro capacity (GW)	Solar capacity (GW)	Wind capacity (GW)
AECI	Associated Electric Cooperative Inc.	Eastern	Midwest	0.03	0.005	1.84
AVA	Avista	Western	Inner West	1.17	0.0384	0.211
BPAT	Bonneville Power Administration	Western	PNW	21.7	0.175	6.6
CISO	Calif. Ind. System Operator	Western	CA	6.46	29.4	11.6
ERCO	Electric Reliability Council of Texas	Texas	Midwest	0.57	9.71	54.7
IPCO	Idaho Power Company	Western	Inner West	2.03	0.633	1.41
ISNE	Ind. System Operator of New England	Eastern	Northeast	1.71	3.03	2.86
LDWP	L.A. Dept. of Water and Power	Western	CA	0.308	1.98	0.677
MISO	Midcontinent Ind. System Operator	Eastern	Midwest	2.4	4.08	52.1
NEVP	Nevada Power Company	Western	Inner West	0.0134	3.19	0.3
NWMT	NorthWestern Energy	Western	Intermountain West	0.681	0.028	0.902
NYIS	New York Ind. System Operator	Eastern	Northeast	4.62	1.32	3.98
PACE	PacifiCorp East	Western	Intermountain West	0.27	2.37	5.11
PACW	PacifiCorp West	Western	PNW	1.13	0.568	1.37
PGE	Portland General Electric	Western	PNW	0.675	0.22	0.899
PJM	PJM Interconnection	Eastern	Northeast	3.31	9.07	19.7
PSCO	Public Service Company of Colo.	Western	Intermountain West	0.0389	1.04	8.38
PSEI	Puget Sound Energy	Western	PNW	0.346	0.001	0.734
SPA	Southwestern Power Authority	Eastern	Midwest	1.51	0.024	0.598
SRP	Salt River Project	Western	Inner West	0.0897	0.518	0.126
SWPP	Southwest Power Pool	Eastern	Midwest	3.08	0.783	47.9
TVA	Tennessee Valley Authority	Eastern	TVA	4.87	0.581	0.0036
WACM	WAPA** - Colorado-Missouri	Western	Intermountain West	0.707	0.381	1.46
WALC	WAPA** - Lower Colorado	Western	Inner West	3.8	0.264	0.7

Table 1: Balancing authorities and their grouping used in this study with hydro, wind, and solar generation capacity represented in this study in gigawatts (GW). The Cluster column indicates the resulting clusters derived from a hierarchical clustering analysis in Section 5.
*North American Electric Reliability Corporation
**Western Area Power Administration

3. Historical properties of seasonal compound VRE drought

In this section we examine the historical frequency, duration, and seasonality of compound VRE droughts in the CONUS. The seasonality and seasonal complementarity of VRE generation can provide insights into when and why compound droughts occur. For example a hypothetical region in which wind, solar and hydropower are perfectly non-complementary, i.e. have identical climotological patterns, would be highly susceptible to seasonal compound drought. Conversely a perfectly complementary region would be highly resilient against compound droughts if capacity are equivalent. Figure 1(a) shows the seasonal climatology of simulated generation from wind, solar, and hydro in each of the BAs in this study. The solid lines represent the median generation expressed as a capacity factor (generation divided by capacity) and the transparent ribbons span the 5th to 95th percentile of monthly generation. While wind and hydro have highly regionally-variable seasonal climotologies, solar presents a similar pattern in almost every BA, peaking in the early summer and falling off in the winter. At the monthly scale, solar also has remarkably low inter-annual variability. Figure 1(b) shows the number of seasonal VRE droughts across all BAs and all years, using a 40th percentile threshold for each resource, where the threshold is based on the monthly values and is fixed across the entire year. Compound droughts are rare in Summer mainly because of the low solar inter-annual variability and strong seasonality, although in some regions seasonally low wind and hydropower also contribute. The Fall is the season most prone to droughts with both the longest duration droughts and highest frequency of occurrence. The fall is when hydro is typically the lowest in both snowmelt and rain driven regions which is consistent with national assessments [56]. Wind can be either climotologically low or high in the fall and winter depending on the region, which, when high, helps to mitigate drought in those seasons in some regions. In Figure 1(c), we can see the spatial pattern of drought frequency: seasonal compound VRE droughts occur the most often in the west with a decreasing frequency moving toward the east. This is primarily due to the lower hydro seasonality and complementarity between wind and solar in these regions.

Figure 2 shows the seasonal distribution of compound VRE droughts from 1982 to 2019 for each BA. In each stacked bar representing the annual total occurrences, the unit bar height is equivalent to one month within a specific season. The distribution over 38 years indicates that the majority of com-

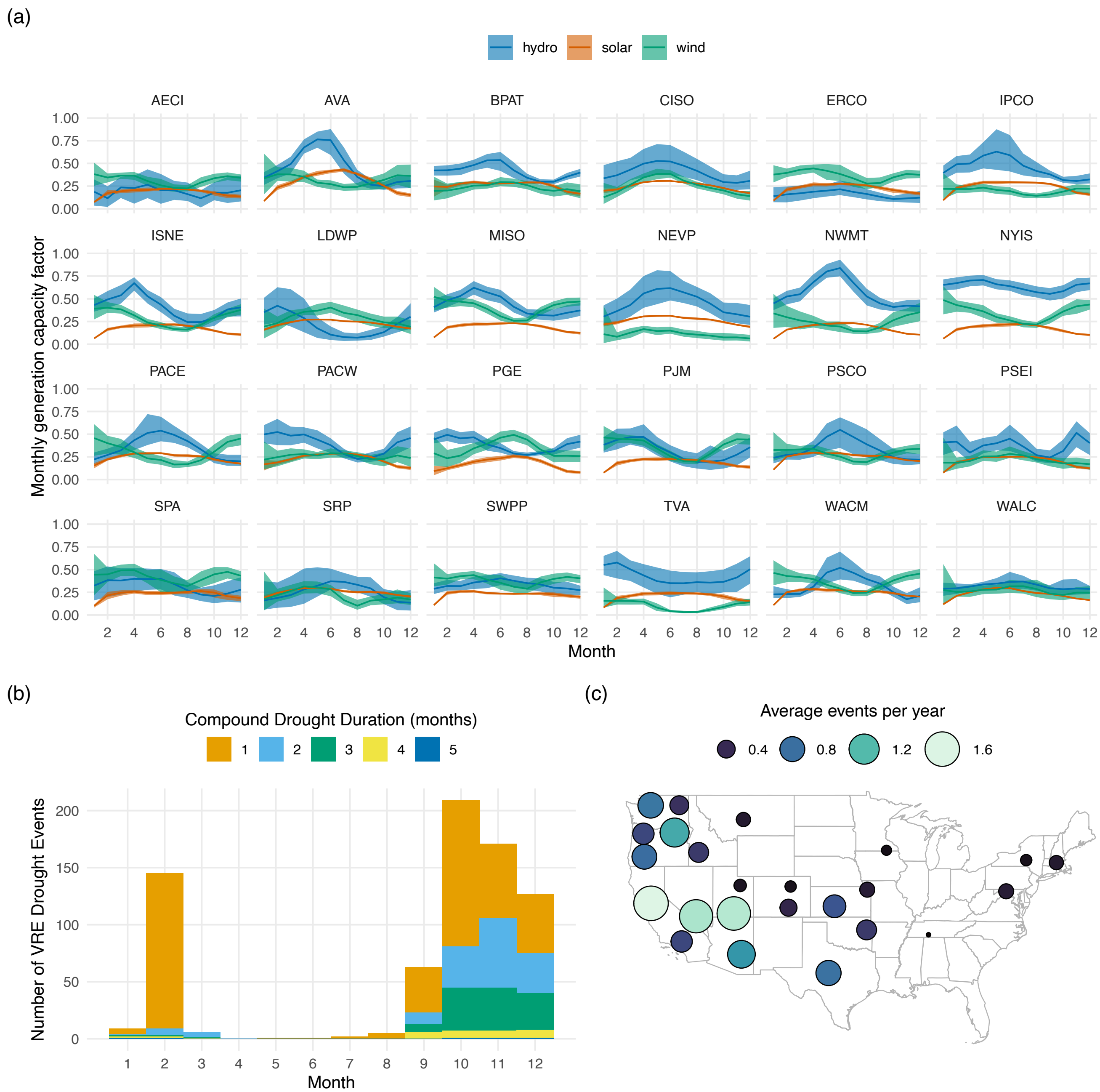

Figure 1: Historical properties of seasonal compound VRE drought: (a) shows the climotological patterns of wind, solar and hydro generation expressed as a capacity factor (generation divided by capacity) for each of the 18 BAs represented in this study. The solid lines represent the median monthly generation and the ribbons span from the 5th to 95th percentiles of the historical period (1982-2018). (b) Shows the seasonal occurrence of compound monthly VRE drought events where the bars are broken down by drought duration in months. (c) Shows the average compound VRE drought frequency for each BA.

pound VRE droughts occur in fall and winter seasons, which is consistent with the previous section and other's findings [33, 37, 5, 38]. Furthermore, these drought events are predominantly concentrated in the Western Interconnection (WI; BPAT to WACM, colored in purple), whereas relatively smaller events are identified in the Eastern Interconnection (EI; AECI to PJM, colored in brown). The WI BAs, including CISO, NEVP, and WALC, experience a significant number of compound drought months during both fall and winter seasons, potentially due to similar low generation patterns across wind, solar and hydro during these seasons, as shown in Figure 1(a). As a result, in these BAs, prolonged VRE droughts from fall to winter could pose a risk to electricity supply, particularly when combined with increased demand driven by winter weather events, such as cold snaps [57]. In contrast, compound VRE droughts are infrequent in the EI BAs, including MISO and TVA, where monthly generation patterns are complementary. A few short-term compound drought months in summer are identified specifically in two EI BAs (SWPP and SPA), which may be linked to intermittent low wind generation with little within-year variation in wind, solar, and hydro generation (Figure 1(a)). Certain BAs (PGE, MISO, TVA, ISNE, NYIS, and PJM) experience compound VRE droughts only during fall. These BAs typically show strong wind or hydro power generation patterns during winter (Figure 1(a)).

4. Seasonal co-occurrence and severity

In an interconnected grid, simultaneous occurrences of compound VRE droughts across BAs may critically impact the bulk power system reliability [58, 4] as adjacent regions are stressed with balancing their demand with their supply shortfall and may have limited regional coordination. Figure 3(a) illustrates the co-occurrences of compound VRE droughts during the fall and winter seasons, with their frequencies represented by the thickness and color of connecting lines between pairs of BAs. Each BA is denoted as a circle, with its size proportional to the total number of VRE drought months, including both isolated and concurrent droughts. In fall, the co-occurrences of compound events are broadly distributed especially within WI BAs, and are temporally aligned with EI BAs despite their lower frequencies. In contrast, during winter, the co-occurrences are particularly pronounced in the southwestern BAs such as CISO, NEVP, WALC, and SRP, with noticeable frequencies extending to limited portions of EI BAs, including AECI, SWPP,

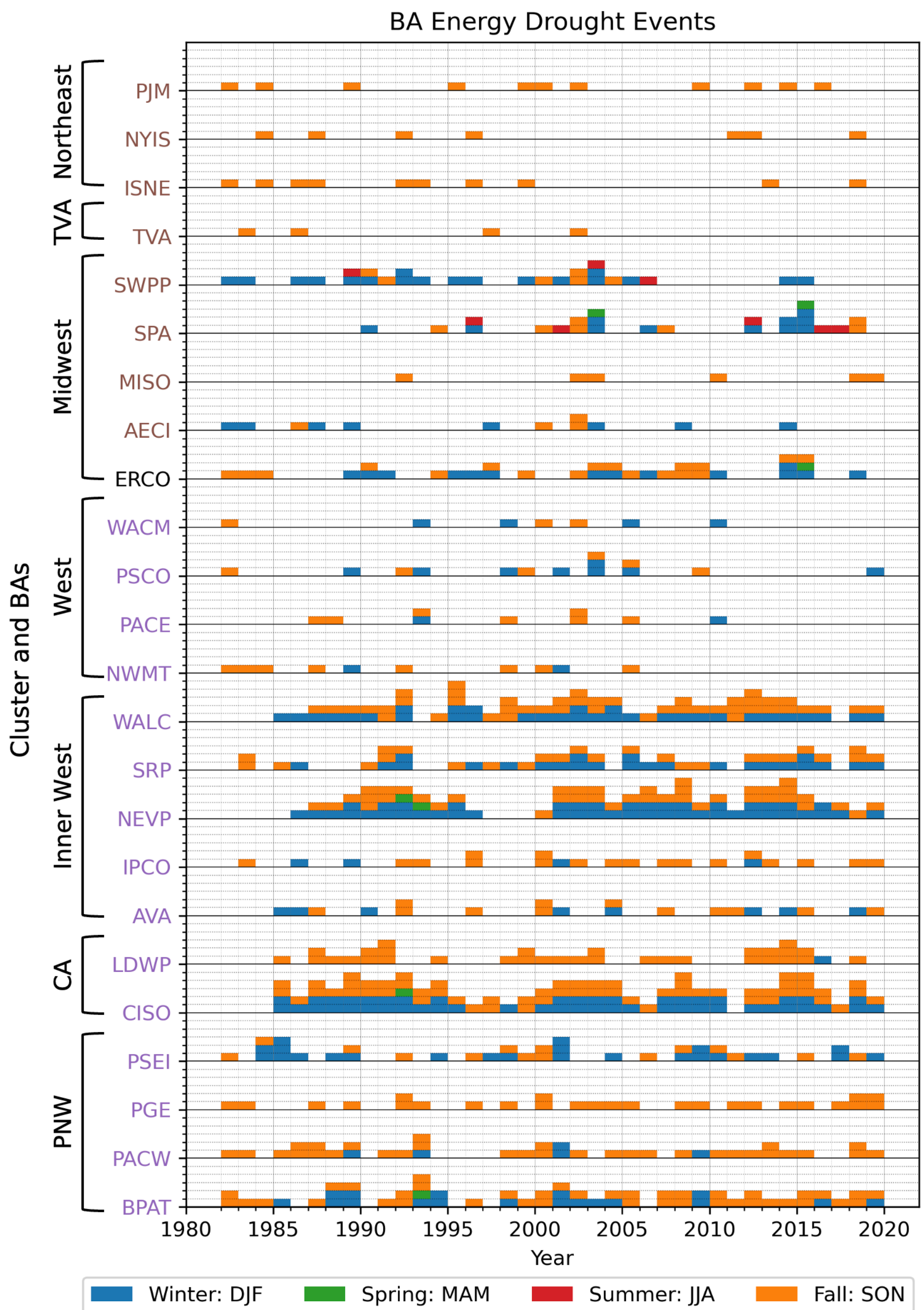

Figure 2: Number of compound energy drought months by season from 1982 to 2019. The unit height of each bar represents one month within a particular season. Note that the BAs in this figure are ordered to align with the clusters from West (bottom) to East (top), detailed in the following sections.

and SPA. The spatial distribution maps for fall and winter indicates two notable trends: a decrease in frequency in the U.S. Pacific Northwest and an increase in frequency in the U.S. southwest and central regions. Consequently, the region vulnerable to coincident resource shortfalls shifts from the western CONUS in fall to the southwestern and central CONUS in winter. These shifts are attributed to regional differences in the seasonality of wind, solar, and hydro generation, as shown in Figure 1(a). However, it is important to note that the concurrent occurrences (connecting lines in Figure 3(a)) do not account for the electricity transmission constraints, which need further consideration to understand their impacts on the interconnected grids. We also note that the Western and Eastern interconnections are not substantially connected however national transmission planning studies explore such opportunities [59], making this regional dependencies even more relevant for cost-benefit analyses.

In the supplementary material, Figure S1 quantifies concurrent VRE drought months between pairs of BAs over 38 years. The lower triangular elements count the co-occurring months of compound droughts during fall, whereas the upper triangular elements count them during winter. Similar to Figure 3(a), a high number of co-occurrences are identified within the WI BAs during fall. The most frequent co-occurrences in fall are between CISO-NEVP (35 months), followed by CISO-WALC (30 months) and CISO-BPAT (30 months). During winter, while the primary locations of co-occurrences remain similar, the CISO-BPAT connection weakens (15 months) and the NEVP-WALC connection strengthens (34 months). Overall, CISO emerges as a hotspot for compound VRE drought during both fall and winter.

As a measure of the combined severity of compound VRE droughts between two BAs, we introduced the concept of severity covariance, which is calculated based on Equation (1):

$$\text{Severity Covariance } (i, j) = \frac{1}{N_D} \sum_{t=1}^{N_D} (z_{i,t} - \overline{z_i})(z_{j,t} - \overline{z_j}) \tag{1}$$

where t represents drought months, z_i and z_j denote the standardized severity indices for a pair of BAs at locations i and j, respectively. N_D is the total number of concurrent VRE drought months, and $\overline{z}$ indicates the mean of the standardized severity indices. Given that the combined severity of VRE droughts is of our primary interest, only the severity indices during drought months (i.e., negative values below the specified threshold) were

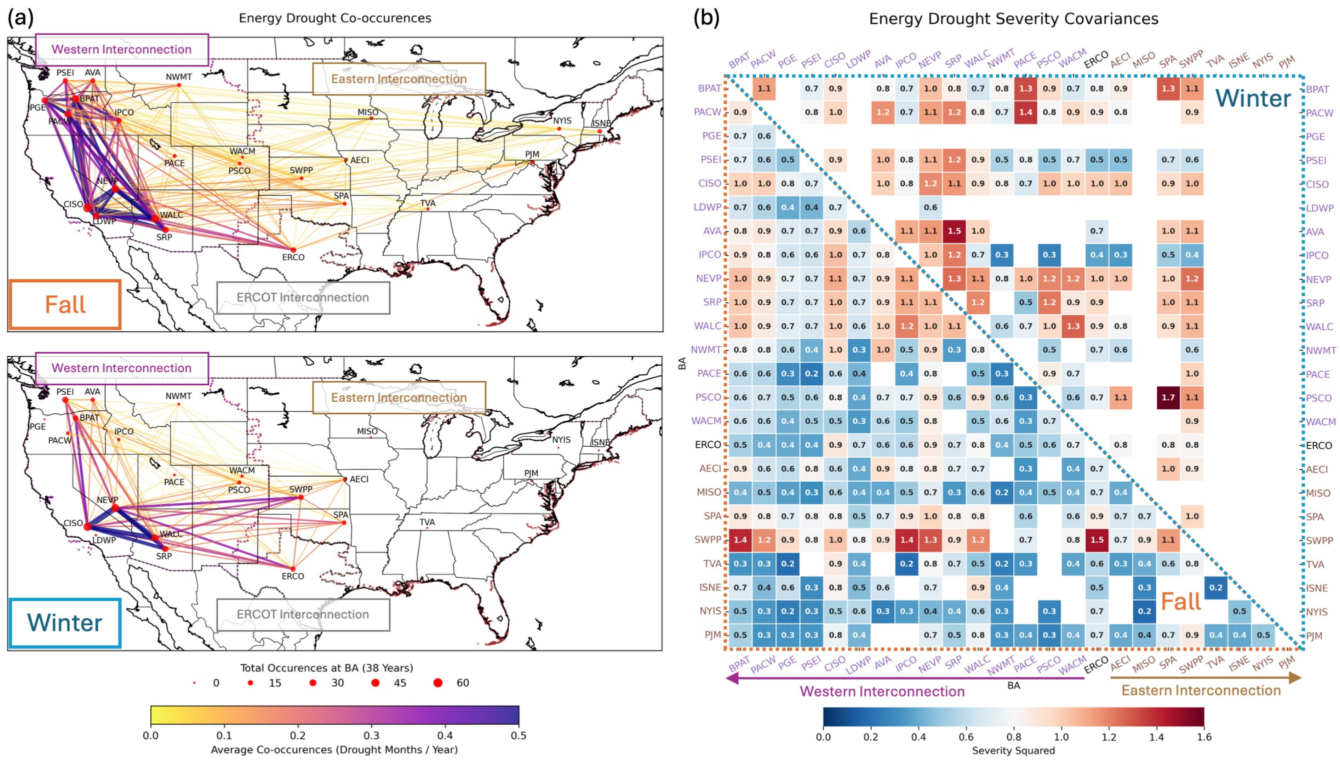

Figure 3: Seasonal patterns of compound VRE droughts: (a) co-occurrence patterns and (b) severity covariance heat map. In panel (a), the circle sizes represent the total number of VRE drought months at BAs, and the connecting line thicknesses indicate the average annual frequency of co-occurrences. The dashed lines delineate the boundaries of Interconnections. In panel (b), the severity covariances for fall and winter are shown in the lower and upper triangular sections, respectively. The BAs are sorted by NERC grid interconnection and Cluster in Table 2.

taken into consideration. In addition, the reference means were set to zero, as the severity indices were derived from standardization to a normal distribution. Therefore, the severity covariances quantify the co-occurring severity trends of compound VRE droughts between pairs of BAs. Figure 3(b) shows a heat map of the severity covariances across BAs. Compared to the co-occurrences heat map in Figure S1, the severity covariances reveal different patterns across BAs and between fall and winter seasons, indicating that the frequency of occurrences is not necessarily correlated with their severity. In winter, although compound VRE droughts are relatively infrequent across the BAs (upper triangular elements of Figure S1), their severity tends to be more intense. Notably, the severity covariance between SPA and PSCO is identified as the highest (1.7 in Figure 3(b)) despite only two co-occurrences over 38 years (two drought months in winter in Figure S1). Specifically, this high severity covariance results from two severe compound events: one driven by hydro droughts in both BAs and the other by low solar production in SPA co-occurring with low hydro generation in PSCO. However, the impact of these severe co-occurrences may be insignificant when considering electricity transmission constraints, as these two BAs are located in different Interconnections. During fall, most BAs tend to undergo relatively frequent (Figure 3(a) and lower triangular elements of Figure S1) but less severe compound VRE droughts, with few exceptions. For example, the primary locations of compound VRE droughts, such as CISO, NEVP, and WALC, show relatively high severity covariance (> 1), in addition to frequent co-occurrences of compound VRE droughts.

5. Climate analysis

This section examines the climate mechanisms driving seasonal compound VRE droughts. Previous studies [37, 2, 11, 60, 16, 33, 32, 12, 14, 23] have demonstrated that seasonal energy droughts are closely related to large-scale atmospheric circulations and climate modes, which typically influence extensive geographic areas and are not confined to specific balancing authority definitions. Many BAs sharing similar geographic locations may be simultaneously affected by the same weather or climate conditions. Therefore, before further investigating the atmospheric conditions inducing these compound VRE droughts, we conduct a hierarchical clustering analysis based on the correlations of the power generations among BAs. As a result, five clusters are generated (Figure 4): (1) PSEI, BPAT, PGE, and PACW; (2) AVA,

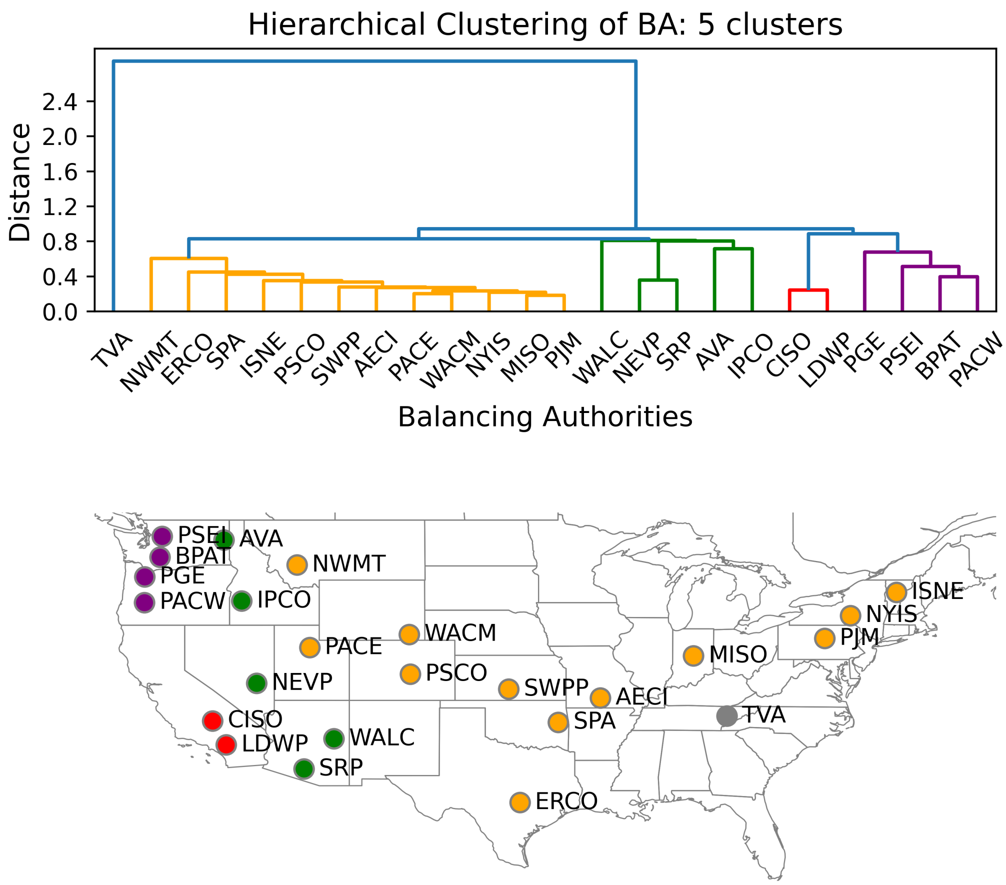

Figure 4: Clustered BAs and their geographic locations.

IPCO, NEVP, WALC, and SRP; (3) CISO and LDWP; (4) TVA; (5) the remaining BAs (Figure S2). Given the geographical extent of the remaining BAs, we further divided them into three groups: the 5th cluster includes NWMT, PACE, WACM, and PSCO; the 6th cluster includes SWPP, SPA, AECI, ERCO, and MISO; the 7th cluster includes PJM, NYIS, and ISNE.

To find the large-scale conditions associated with droughts for given clustered BAs, we selected large-scale variables, including 500 hPa geopotential height, sea surface data, mean sea level pressure, relative humidity, temperature, and wind at the surface, 850 hPa, 500 hPa, and 200 hPa. We further composited the monthly anomaly of each variable by removing the climatological monthly mean between 1982 and 2019 for each from ERA5 monthly averaged reanalysis data [43, 61]. After clustering the BAs, we found that historically the number of seasonal droughts events range from 4 for the TVA cluster to a larger sample size for other clusters. To conduct a fair composite analysis (averaging the anomalies for each cluster), we limited each cluster to the top 4 events for the purposes of calculating the climatological anomalies. Therefore, for TVA, we averaged all the drought months in the composite analysis; for other clusters, we selected the four months with the most severe drought indices.

For this study, we also calculated the correlation between power generation and the Arctic Oscillation (AO), the North Atlantic Oscillation (NAO), and the El Niño-Southern Oscillation (ENSO) Precipitation Index (ESPI). 5 shows the correlation coefficients between power generation and climate indices for each BA. While individual energy resources within these clusters may show correlations with climate indices, the aggregate power generation for these clusters does not always exhibit such relationships

For the PNW (PSEI, BPAT, PGE, and PACW) cluster, wind energy is the dominant renewable energy source, and it shows a strong correlation with the ESPI index. Additionally, the AO is correlated with power generation in two BAs within this cluster: BPAT and PACW. Due to the predominant role of wind energy, the correlation between wind energy and ESPI also drives the compound total power generation for this cluster. Furthermore, hydropower generation for PGE and PACW exhibits some correlations with the ESPI index.

In the CA (CISO and LDWP) cluster, there are minimal correlations between power generation and the three climate indices (AO, NAO, and ESPI). The only notable correlations are between hydropower generation for CISO with ESPI and NAO.

The Inner West (AVA, IPCO, NEVP, WALC, and SRP) cluster also shows rare coherent correlations. NAO is correlated with both solar and hydro generation for WALC, while ESPI is correlated with hydropower generation for NEVP and with wind energy for SRP.

The Intermountain West (NWMT, PACE, WACM, and PSCO) cluster is predominantly wind energy-focused, but there is little evidence showing strong correlations between solar or hydropower and climate indices. The correlation with wind energy influences the cluster's total energy generation. However, the only significant correlation observed within this cluster is between NAO and wind generation for NWMT

The Midwest (SWPP, SPA, AECI, ERCO, and MISO) cluster exhibits different behaviors. While some significant correlations exist between single-source generation (e.g., solar and hydropower) and climate indices, these correlations are not evident in compound power generation. ESPI is correlated with solar generation for SWPP and with hydropower generation for other BAs in this cluster. NAO is highly correlated with solar overall, and AO shows correlation with hydropower generation for SWPP. However, there is no evident correlation between wind energy and the climate indices.

In the NE (PJM, NYIS, and ISNE) cluster, there is a high correlation between NAO and solar generation across the entire cluster, as well as between NAO and hydropower generation for PJM. Similar to the fifth cluster, there is no evident correlation between wind generation and climate indices, and the correlation rarely appears in the compound total energy.

The pattern in the TVA cluster is very similar to that in the NE cluster, with the exception that hydropower generation shows a correlation with ESPI.

Note that the Intermountain West, Midwest, and NE clusters are separated artificially; initially, they formed one larger cluster based on total power generation 4. This separation can be traced by no significant correlation with climate indices across these three clusters, except for the NAO in the case of NWMT.

The investigation into the weather mechanisms driving the occurrence of seasonal energy droughts across various regions highlights important atmospheric variables influencing energy resources. However, the direct application of these weather pattern descriptions for predictability remains challenging. For example, while we observe that an Arctic Ridge pattern can be associated with drought conditions in the Pacific Northwest (PNW: PSEI, BPAT, PGE, and PACW) cluster, it is not necessarily the case that every Arctic Ridge event results in a drought, nor is the duration of the Arctic Ridge always sufficient to establish a clear and robust causality.

To strengthen the focus on predictability, we have concentrated on regions where we have identified clear causality between climate indices and renewable energy droughts. For instance, our analysis shows that in the California (CA: CISO and LDWP) cluster, specific climate indices such as the El Niño Southern Oscillation have a significant correlation with hydropower generation deficits. Detailed discussions and analyses of these regions with clear causality are provided in the supplementary material.

We acknowledge that the qualitative descriptions of weather patterns in other regions require further research to establish their predictive capability.

Therefore, we have moved the detailed composite analyses of these regions to the supplementary material. This allows us to maintain a clear focus in the main text on regions where predictability based on climate indices is more established.

6. Case Study

This section presents a case study of the potential impacts of these seasonal compound VRE droughts on grid operations in the western U.S. These impacts are studied on the WI using the WECC 2030 Anchor Data Set (ADS) Gridview test case. GridView, a grid operations model widely utilized in the industry, is used to model the behavior of dispatch. A full year in hourly resolution, at the nodal scale, is modeled for six scenarios. The first is presented as a control, and corresponds to a normal, non-drought year. The other scenarios correspond to drought events that were selected to represent the worst historical drought conditions across the entire WI. These are referred to as "Event 1" through "Event 5", where Event 1 is the most extreme overall and Event 5 is the least extreme. Five months from different years were identified that had the largest compound VRE drought severity across all BAs in the WI where the severity is defined as the total energy deficit below the 40th percentile drought threshold. Any BA drought that overlapped with the identified month was also captured in the input datasets for the GridView model. The droughts were used to modify the WECC 2030 ADS test case by proportionally lowering the VRE generation according to the historical generation during the identified droughts. For example if the wind in a BA had an average monthly capacity factor of 0.2 during a drought month and the WECC 2030 ADS had an average monthly capacity factor of 0.4, then the hourly generation of all plants in the BA would be lowered by 50% to account for the drought conditions.

It is expected that drought years, as compared to typical years, will stress the grid in some way. In particular, reduced generation from solar, wind, and hydro, is expected to either reduce reliability, or increase dependence on gas resource. In practice, the WECC 2030 ADS features a robust generation portfolio. For this analysis, no resource adequacy concerns, such as unserved energy, are observed. Still, in less robust test cases, unserved energy may be a concern.

Even without unserved energy, droughts still impose notable impacts on grid operations. Figure 6 shows the increase in emissions and locational

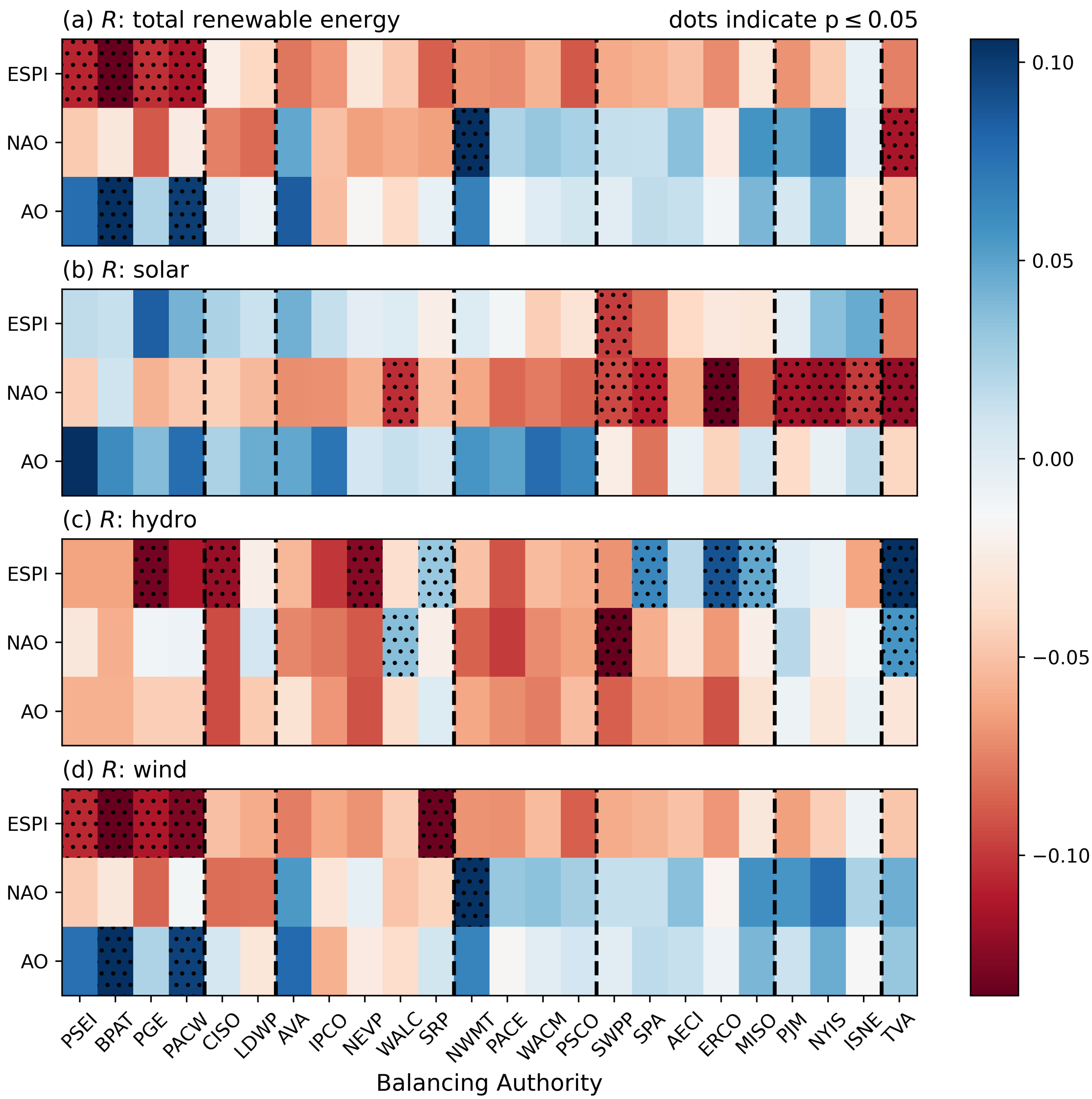

Figure 5: Heat map of the correlation (R) between power generation and climate indexes for each BA. Note that the black dots indicate that the correlation is statistically significant when the p-value is less than the significance level of 0.05; the dashed lines between BAs indicate different clusters for BAs. (a) is for total power energy generation, (b) is for solar, (c) is for hydropower, and (d) is for wind generations.

marginal prices (LMPs) that exhibited during the drought as opposed to normal operation. For the sake of this analysis, the averages are computed and compared across the extent of the drought in question with the normal, non-drought year. This separates the impact of the drought from normal annual variations in the behavior of these features. In general, drought events are associated with a modest impact in the emissions. However, in some cases, droughts result in spikes of the zonal emissions by well over 20% which is in line with Voisin et al.[23] who showed that hydropower drought alone can contribute to 10% increased emissions. This points towards the reduced generation due to drought being compensated for using gas-fired power plants.

Locational marginal prices (LMPs) convey the price of energy at a particular spatial location. In essence, they encode the availability of energy, and are a function of several factors including fuel costs and transmission congestion. Intuitively, droughts increase reliance on gas generation to serve demand, thus leading to higher fuel component of LMPs. This behavior is most heavily concentrated in the Northwest with LMPs increasing by 5-10% in every event. Some regions actually have 5-10% lower LMPs during the drought. This is due to reduced renewable and hydro generation resulting in less transmission congestion, and thus lower congestion component of the LMP.

7. Discussion

The analysis of monthly timescale VRE droughts require long term climate simulations, representation of land surface processes and human systems dynamics. Seasonal compound VRE droughts in the contiguous U.S. have diverse regional characteristics that stem from the complementarity of the wind, solar and hydro generation. In the CISO BA (California), these three renewable resources are almost perfectly non-complementary and consequently we see that region with the highest frequency of compound VRE drought. Conversely in the TVA BA (Tennessee), wind and hydro are almost perfectly complementary with solar and in that BA we see the lowest frequency of compound VRE drought. Furthermore, very few droughts occur in the summer in any BA which is driven by both the high solar and high hydro in the western U.S. Analogously, fall is the most prone to compound VRE droughts due to low hydro and tapering off solar. Wind tends not to be an overall driver of compound VRE drought due to how variable it is across regions. Based on these results we can conclude that climatological comple-

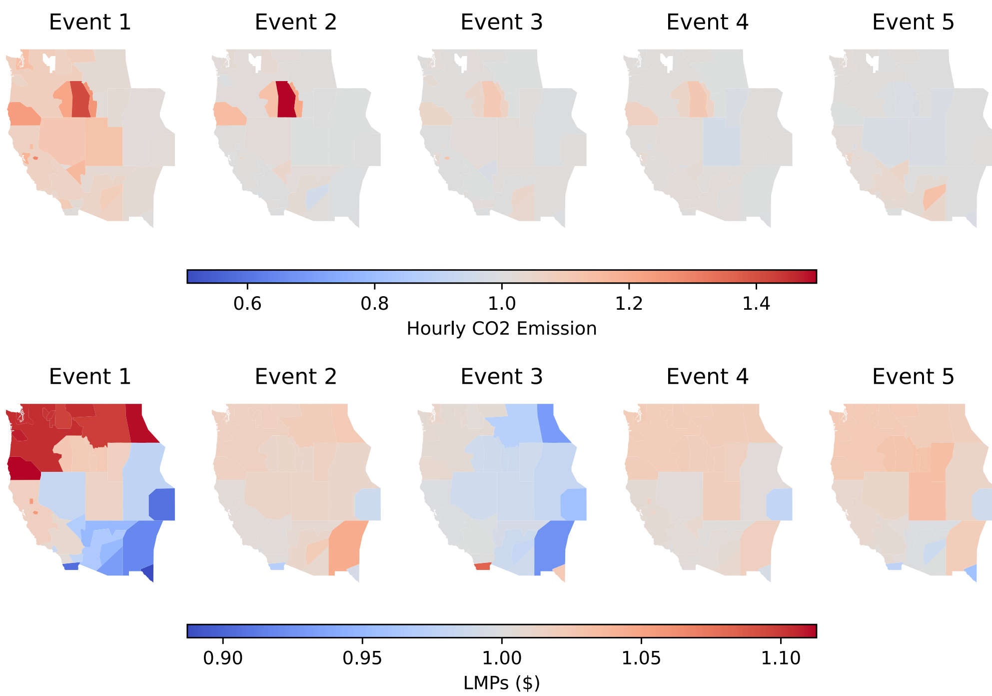

Figure 6: Average emission ratio (top row) and average locational marginal price (bottom row) of each compound drought event divided by the baseline scenario (positive values indicate an increase in the energy drought scenario).

mentarity is the main driver of the seasonal occurrence and frequency of VRE droughts at the monthly timescale. This insight indicates that climatology is a good indication to guide the development of renewable energy. While this is already performed in practice for individual resources, the insight further informs balancing regions in how to promote sustainable growth with a strategic distribution of capacities across the different resources. Many long term planning electricity models - also called capacity expansion models, often have a simplified representation of sub-annual dynamics with representative seasonal "stress periods". This study emphasizes the need to represent the complementarity between the renewable resources across all seasons and not select individual wind-solar-hydro supply curves which might lead to over building.

The spatial co-occurrences and co-severity of compound VRE droughts among BAs can provide valuable insights into the extent and intensity of their seasonal occurrences concentrated in specific regions. This aspect is critical to inform coordination across balancing regions with the exploration of new transmission path or re-sizing of the existing capacity. This co-occurrence can also inform the development of long term contracts across balancing regions. The primary regions of co-occurrences shift from the Western Interconnect BAs (CA, PNW, and Inner West clusters) in fall to the southwestern BAs (CA, Inner West, and Midwest clusters) in winter, due to the different seasonal responses of solar, wind, and hydro generation by region. Particularly, the BAs in California (CISO), Nevada (NEVP), and Arizona (WALC) experience persistent co-occurrences of compound VRE droughts throughout both fall and winter. Based on these seasonal shifts around surrounding BAs, power system planning for compound VRE droughts could be optimized by considering spatial complementarity together with electricity transmission constraints and load seasonality also needs to be considered. Furthermore, the severity covariance matrix informs the historical patterns of the concurrent intensity, which could be further integrated into power system planning to address deficiencies in electricity supply. The calculations of the severity covariances reveal that co-occurrences do not necessarily correlate with severity, as demonstrated by the BAs, which experience smaller but more intense events in winter. It is important to note that the correlation and covariance information provides only spatiotemporal alignment in the frequency and severity of compound VRE droughts, without accounting for the relative scales of electricity generation by energy source. This aspect may be important for the practical planning of power system grids.

The clustering analysis based on power generation correlations among BAs reveals a complex picture. Some BAs have one or two renewable energy sources which are strongly correlated to climate indices, while others have none. Although the total energy generation was utilized for clustering analysis, the lack of correlation of specific resource may or may not propagate to influence the total energy generation, depending on the relative amount of each generation in each region. As a result, climate characteristics are unlikely to fully explain the occurrence of compound droughts; rather, they provide insight into the predictability of certain energy sources in specific regions. This phenomenon is particularly evident in regions such as the Pacific Northwest, which has abundant wind and hydropower resources, but limited solar power, and TVA, where solar and hydropower are plentiful but wind resources are minimal. Future studies should conduct detailed regional analyses to better understand the underlying mechanisms driving energy droughts and conclude on their predictability.

Studying single-resource energy droughts focuses on the impact of climate variability on individual renewable energy sources, allowing for clearer identification of climate drivers and more straightforward mitigation strategies. For instance, analyzing wind energy droughts in isolation can directly link specific atmospheric circulation patterns, such as weather regimes (WRs), to wind speed anomalies. However, compound energy droughts involve the simultaneous deficit of multiple energy sources, adding complexity to the analysis. These compound events are influenced by a multitude of interacting climate variables and local factors, and our composite analysis reveals that specific weather patterns are indeed associated with energy compound droughts. This indicates that understanding these patterns can enhance forecasting and energy planning. Understanding the key differences between single and compound energy droughts is crucial for developing resilient energy systems and improving forecasting methods that accurately account for the combined effects of different renewable energy sources.

The resource adequacy case study demonstrated that the planned 2030 infrastructure for the Western US would be robust to compound energy droughts with enough gas generation capacity held to meet demand in even the most extreme compound VRE droughts. The WECC 2030 ADS case dates back to 2020 when governmental policies were not targeting a substantial shift in energy generation portfolio and had a low end of wind and solar penetration with respect to other projections [62, 63, 59]. We anticipate that this library of compound wind-solar-hydro drought events will have a growing interest as the generation portfolio includes more of those resources. We also note that this library of events to guide resource adequacy studies needs to be complemented with the consideration for the load seasonality. For example, Yates et al.[64] demonstrated that the California irrigation load increase by 6 percent in times of hydrological drought when hydropower resources are reduced by 20 percent. In addition, energy storage is recognized as a critical fleet component for shifting energy from hours with plentiful generation to hours with high load. In the case of seasonal droughts, long term duration energy storage with time scale of weeks and months may be necessary to maintain grid reliability and price volatility.

8. Limitations

One limitation of this study is that load was not considered along side generation. Considering load is important for resource adequacy considerations at this time scale. For example, Fall was identified as the season with the most likely compound VRE drought events, but this season typically has mild temperatures in the US so the grid impacts of such events are uncertain. To quantify the true grid impacts, load and transmission constraints should be considered in future studies. To fully quantify these impacts, a bulk power system model, such as a capacity expansion model or a unit commitment economic dispatch model, is necessary.

Our results indicate some inconsistency between hydropower energy deficits and their climate proxies (IWV and VPD), particularly in regions like the TVA, Midwest, Intermountain, and Inner West. Hydropower is subject to human management, especially for dams where the occurrence of hydropower droughts is linked to atmospheric and hydrological drought conditions over extended periods of time. An accurate explanation of the connection between hydropower droughts and climate requires examining much longer timescales, often multiple years. Therefore, a minimum time span must be established to effectively use climate and weather patterns to explain hydropower droughts. Additionally, since the time scales of wind and solar are much shorter it would be beneficial to find an approach which allows for each resource to be included at the time scale with the most impact, such as a wind and solar drought during a heat wave which occurs during a period of hydrologic drought.

9. Conclusion

This study provides an analysis of compound wind, solar and hydropower seasonal energy droughts across the contiguous Unites States. Hydropower is by far the most complex component of the renewable droughts, requiring climate, land surface and water management modeling. Hydropower necessarily operates at a different timescale than wind or solar, necessitating a longer seasonal view of variable renewable droughts and strategies in managing multiple water uses. At this seasonal timescale, weather variability becomes less important than the climatological complementarity of generation resources. Regions which have highly complementary resources for similar generating capacities will experience less compound drought and visa-versa. While this is an intuitive result, it is important to quantify to aid in regional planning and to prevent overbuilding. Additionally, our analysis identifies transmission-connected regions which have high risk for compound variable renewable energy droughts to co-occur, which can support transmission planning adequacy and reliability studies.

Our climate analysis has indicated that predicting certain renewable sources at the seasonal scale may be possible in some regions of the contiguous United States. The atmospheric conditions which lead to compound droughts are complex and prediction of these compound events will require further study.

The case study presented serves as an example of how renewable energy drought data can be incorporated into production cost models to determine energy prices, transmission congestion, and carbon emissions during renewable drought events. Our results indicated that the modeled 2030 infrastructure was robust in the sense there was no unserved energy but this may change as wind and solar are rapidly developed. The compound droughts we identified using coincident data may serve as a new baseline for resource adequacy planning. While coincident wind-solar-load datasets are necessary for reliability studies and understand storage and reserve needs, this study indicates that hydropower drought conditions may be paired with other wind-solar-load datasets for the purpose of evaluating compound multi-scale extreme events, in some regions like the snowmelt dominated Western US. Such mix and match requires further evaluation and are scale-dependent and the provided analytics can support such regional evaluation.

10. Data Availability

The data used in this paper is available on Zenodo: `https://zenodo.org/records/14270835`. The code used to conduct the analysis and produce figures is available on GitHub: `https://github.com/GODEEEP/seasonal-energy-droughts`.

11. Acknowledgments

This research was supported by the Grid Operations, Decarbonization, Environmental and Energy Equity Platform (GODEEEP) Investment, under the Laboratory Directed Research and Development (LDRD) Program at Pacific Northwest National Laboratory (PNNL). The study leverages the TGW climate datasets developed by U.S. DOE Office of Science multisector dynamics program as part of the IM3 and HyperFACETS projects. This work leverages the capabilities of mosartwmpy, a Python version of the MOSART-WM model supported by the U.S. Department of Energy, Office of Science, as part of research in MultiSector Dynamics, Earth, and Environmental Systems Modeling Program and enhanced by the Energy Efficiency and Renewable Energies - Hydrological Sciences Program. This work also leverages early formulation developed under the HydroWIRES B1 project (grant 75563) sponsored by the Water Power Technologies Office under the HydroWIRES initiative. This research used resources of the Pacific Northwest Research Computing at the PNNL, which is a DOE Office of Science User Facility. The PNNL is a multi-program national laboratory operated by Battelle Memorial Institute for the U.S. Department of Energy (DOE) under Contract No. DE-AC05-76RL01830. Accordingly, the U.S. Government retains and the publisher, by accepting the article for publication, acknowledges that the U.S. Government retains a nonexclusive, paid-up, irrevocable, worldwide license to publish or reproduce the published form of this manuscript or allow others to do so, for U.S. Government purposes.

References

[1] D. Raynaud, B. Hingray, B. François, J. D. Creutin, Energy droughts from variable renewable energy sources in european climates, Renewable Energy 125 (2018) 578–589. doi:https://doi.org/10.1016/j.renene.2018.02.130.

[2] N. Otero, O. Martius, S. Allen, H. Bloomfield, B. Schaefli, Characterizing renewable energy compound events across europe using a logistic regression-based approach, Meteorological Applications 29 (5) (2022) e2089. doi:https://doi.org/10.1002/met.2089.

[3] N. Otero, O. Martius, S. Allen, H. Bloomfield, B. Schaefli, A copula-based assessment of renewable energy droughts across europe, Renewable Energy 201 (2022) 667–677. doi:https://doi.org/10.1016/j.renene.2022.10.091.

[4] C. Bracken, N. Voisin, C. D. Burleyson, A. M. Campbell, Z. J. Hou, D. Broman, Standardized benchmark of historical compound wind and solar energy droughts across the continental united states, Renewable Energy 220 (2024) 119550. doi:https://doi.org/10.1016/j.renene.2023.119550.

[5] D. Richardson, A. J. Pitman, N. N. Ridder, Climate influence on compound solar and wind droughts in australia, npj Climate and Atmospheric Science 6 (1) (Nov. 2023). doi:https://doi.org/10.1038/s41612-023-00507-y.

[6] H. Lei, P. Liu, Q. Cheng, H. Xu, W. Liu, Y. Zheng, X. Chen, Y. Zhou, Frequency, duration, severity of energy drought and its propagation in hydro-wind-photovoltaic complementary systems, Renewable Energy 230 (2024) 120845. doi:https://doi.org/10.1016/j.renene.2024.120845.

[7] V. Gburčik, S. Mastilović, Željko Vučinić, Assessment of solar and wind energy resources in serbia, Journal of Renewable and Sustainable Energy 5 (4) (2013) 041822. doi:https://doi.org/10.1063/1.4819504.

[8] P. E. Bett, H. E. Thornton, The climatological relationships between wind and solar energy supply in britain, Renewable Energy 87 (2016) 96–110. doi:https://doi.org/10.1016/j.renene.2015.10.006.

[9] M. M. Miglietta, T. Huld, F. Monforti-Ferrario, Local complementarity of wind and solar energy resources over europe: An assessment study from a meteorological perspective, Journal of Applied Meteorology and Climatology 56 (1) (2017) 217–234. doi:https://doi.org/10.1175/jamc-d-16-0031.1.

[10] B. François, B. Hingray, D. Raynaud, M. Borga, J. D. Creutin, Increasing climate-related-energy penetration by integrating run-of-the river hydropower to wind/solar mix, Renewable Energy 87 (2016) 686–696. doi:https://doi.org/10.1016/j.renene.2015.10.064.

[11] K. van der Wiel, H. C. Bloomfield, R. W. Lee, L. P. Stoop, R. Blackport, J. A. Screen, F. M. Selten, The influence of weather regimes on european renewable energy production and demand, Environmental Research Letters 14 (9) (2019) 094010. doi:https://doi.org/10.1088/1748-9326/ab38d3.

[12] M. Gonzalez-Salazar, W. R. Poganietz, Making use of the complementarity of hydropower and variable renewable energy in latin america: A probabilistic analysis, Energy Strategy Reviews 44 (2022) 100972. doi:https://doi.org/10.1016/j.esr.2022.100972.

[13] J. A. Ferraz de Andrade Santos, P. de Jong, C. Alves da Costa, E. A. Torres, Combining wind and solar energy sources: Potential for hybrid power generation in brazil, Utilities Policy 67 (2020) 101084. doi:https://doi.org/10.1016/j.jup.2020.101084.

[14] H. C. Bloomfield, C. M. Wainwright, N. Mitchell, Characterizing the variability and meteorological drivers of wind power and solar power generation over africa, Meteorological Applications 29 (5) (2022) e2093. doi:https://doi.org/10.1002/met.2093.

[15] P. T. Brown, D. J. Farnham, K. Caldeira, Meteorology and climatology of historical weekly wind and solar power resource droughts over western north america in ERA5, SN Applied Sciences 3 (10) (sep 2021). doi:https://doi.org/10.1007/s42452-021-04794-z.

[16] K. Doering, S. Steinschneider, Summer covariability of surface climate for renewable energy across the contiguous united states: Role of the north atlantic subtropical high, Journal of Applied Meteorology and Climatology 57 (12) (2018) 2749–2768. doi:https://doi.org/10.1175/jamc-d-18-0088.1.

[17] K. Z. Rinaldi, J. A. Dowling, T. H. Ruggles, K. Caldeira, N. S. Lewis, Wind and solar resource droughts in california highlight the benefits of long-term storage and integration with the western intercon-

nect, Environmental Science & Technology 55 (9) (2021) 6214–6226. doi:https://doi.org/10.1021/acs.est.0c07848.

[18] Y. Amonkar, D. J. Farnham, U. Lall, A k-nearest neighbor space-time simulator with applications to large-scale wind and solar power modeling, Patterns 3 (3) (2022) 100454. doi:https://doi.org/10.1016/j.patter.2022.100454.

[19] D. Zheng, D. Tong, S. J. Davis, Y. Qin, Y. Liu, R. Xu, J. Yang, X. Yan, G. Geng, H. Che, Q. Zhang, Climate change impacts on the extreme power shortage events of wind-solar supply systems worldwide during 1980–2022, Nature Communications 15 (1) (Jun. 2024). doi:https://doi.org/10.1038/s41467-024-48966-y.

[20] M. Ghosal, A. M. Campbell, M. A. Elizondo, N. A. Samaan, Q. H. Nguyen, T. B. Nguyen, C. Munõz, D. M. Hernandéz, Grid reserve and flexibility planning tool (graf-plan) for assessing resource balancing capability under high renewable penetration, IEEE Open Access Journal of Power and Energy 10 (2023) 560–571. doi:https://doi.org/10.1109/OAJPE.2022.3169729.

[21] O. J. Guerra, J. Zhang, J. Eichman, P. Denholm, J. Kurtz, B.-M. Hodge, The value of seasonal energy storage technologies for the integration of wind and solar power, Energy & Environmental Science 13 (7) (2020) 1909–1922. doi:https://doi.org/10.1039/D0EE00771D.

[22] A. Zeighami, J. Kern, A. J. Yates, P. Weber, A. A. Bruno, U.s. west coast droughts and heat waves exacerbate pollution inequality and can evade emission control policies, Nature Communications 14 (1) (Mar. 2023). doi:https://doi.org/10.1038/s41467-023-37080-0.

[23] N. Voisin, M. Kintner-Meyer, D. Wu, R. Skaggs, T. Fu, T. Zhou, T. Nguyen, I. Kraucunas, Opportunities for joint water–energy management: Sensitivity of the 2010 western u.s. electricity grid operations to climate oscillations, Bulletin of the American Meteorological Society 99 (2) (2018) 299–312. doi:https://doi.org/10.1175/bams-d-16-0253.1.

[24] F. A. Wolak, Long-term resource adequacy in wholesale electricity markets with significant intermittent renewables, Environmental and Energy

Policy and the Economy 3 (2022) 155–220. doi:https://doi.org/10.1086/717221.

[25] R. Schroeder, A. Joyeau, E. M. Carlini, Seasonal adequacy risks, in: 2018 IEEE International Conference on Environment and Electrical Engineering and 2018 IEEE Industrial and Commercial Power Systems Europe (EEEIC / I&CPS Europe), IEEE, 2018, pp. 1–6. doi:10.1109/eeeic.2018.8494396.

[26] B. François, H. Puspitarini, E. Volpi, M. Borga, Statistical analysis of electricity supply deficits from renewable energy sources across an alpine transect, Renewable Energy 201 (2022) 1200–1212. doi:https://doi.org/10.1016/j.renene.2022.10.125.

[27] L. v. d. Most, K. v. d. Wiel, W. Gerbens-Leenes, R. R. Benders, R. Bintanja, Temporally compounding energy droughts in european electricity systems with hydropower, Nature Energy (Jan. 2024). doi:https://doi.org/10.21203/rs.3.rs-3796061/v1.

[28] A. Wörman, I. Pechlivanidis, D. Mewes, J. Riml, C. Bertacchi Uvo, Spatiotemporal management of solar, wind and hydropower across continental europe, Communications Engineering 3 (1) (Jan. 2024). doi:https://doi.org/10.1038/s44172-023-00155-3.

[29] A. Somani, S. Datta, S. Kincic, V. Chalishazar, B. Vyakaranam, N. Samaan, A. Colotelo, Y. Zhang, V. Koritarov, T. McJunkin, T. Mosier, J. Novacheck, M. Emmanuel, M. Schwarz, L. Markel, C. O'Reilley, Hydropower's contributions to grid resilience, Tech. rep., Pacific Northwest National Laboratory (2021).

[30] D. Tong, D. J. Farnham, L. Duan, Q. Zhang, N. S. Lewis, K. Caldeira, S. J. Davis, Geophysical constraints on the reliability of solar and wind power worldwide, Nature Communications 12 (1) (2021) 6146. doi:https://doi.org/10.1038/s41467-021-26355-z.

[31] K. Engeland, M. Borga, J.-D. Creutin, B. François, M.-H. Ramos, J.-P. Vidal, Space-time variability of climate variables and intermittent renewable electricity production – a review, Renewable and Sustainable Energy Reviews 79 (2017) 600–617. doi:https://doi.org/10.1016/j.rser.2017.05.046.

[32] K. Mohammadi, N. Goudarzi, Study of inter-correlations of solar radiation, wind speed and precipitation under the influence of el niño southern oscillation (enso) in california, Renewable Energy 120 (2018) 190–200. doi:https://doi.org/10.1016/j.renene.2017.12.069.

[33] L. Lledó, O. Bellprat, F. J. Doblas-Reyes, A. Soret, Investigating the effects of pacific sea surface temperatures on the wind drought of 2015 over the united states, Journal of Geophysical Research: Atmospheres 123 (10) (2018) 4837–4849. doi:https://doi.org/10.1029/2017JD028019.

[34] K. van der Wiel, L. Stoop, B. van Zuijlen, R. Blackport, M. van den Broek, F. Selten, Meteorological conditions leading to extreme low variable renewable energy production and extreme high energy shortfall, Renewable and Sustainable Energy Reviews 111 (2019) 261–275. doi:https://doi.org/10.1016/j.rser.2019.04.065.

[35] H. C. Bloomfield, D. J. Brayshaw, A. J. Charlton-Perez, Characterizing the winter meteorological drivers of the european electricity system using targeted circulation types, Meteorological Applications 27 (1) (2020) e1858. doi:https://doi.org/10.1002/met.1858.

[36] H. C. Bloomfield, C. C. Suitters, D. R. Drew, Meteorological drivers of european power system stress, Journal of Renewable Energy 2020 (2020) 5481010. doi:https://doi.org/10.1155/2020/5481010.

[37] Y. Liu, S. Feng, Y. Qian, H. Huang, L. K. Berg, How do north american weather regimes drive wind energy at the sub-seasonal to seasonal timescales?, npj Climate and Atmospheric Science 6 (1) (Jul. 2023). doi:https://doi.org/10.1038/s41612-023-00403-5.

[38] X. Yang, T. L. Delworth, L. Jia, N. C. Johnson, F. Lu, C. McHugh, Skillful seasonal prediction of wind energy resources in the contiguous united states, Communications Earth & Environment 5 (1) (Jun. 2024). doi:https://doi.org/10.1038/s43247-024-01457-w.

[39] M. Kittel, W.-P. Schill, Measuring the dunkelflaute: How (not) to analyze variable renewable energy shortage, Environmental Research: Energy (Aug. 2024). doi:https://doi.org/10.1088/2753-3751/ad6dfc.

[40] C. Bracken, Y. Son, D. Broman, N. Voisin, Godeeep-hydro: Historical and projected power system ready hydropower data for the united states, Scientific Data (2024).

[41] A. D. Jones, D. Rastogi, P. Vahmani, A. M. Stansfield, K. A. Reed, T. Thurber, P. A. Ullrich, J. S. Rice, Continental united states climate projections based on thermodynamic modification of historical weather, Scientific Data 10 (1) (sep 2023). doi:https://doi.org/10.1038/s41597-023-02485-5.

[42] W. C. Skamarock, J. B. Klemp, J. Dudhia, D. O. Gill, Z. Liu, J. Berner, W. Wang, J. G. Powers, M. G. Duda, D. M. Barker, X.-Y. Huang, A description of the advanced research wrf model version 4, Report, National Center for Atmospheric Research (2019). doi:10.5065/1dfh-6p97. URL http://dx.doi.org/10.5065/1dfh-6p97

[43] H. Hersbach, B. Bell, P. Berrisford, S. Hirahara, A. Horányi, J. Muñoz-Sabater, J. Nicolas, C. Peubey, R. Radu, D. Schepers, A. Simmons, C. Soci, S. Abdalla, X. Abellan, G. Balsamo, P. Bechtold, G. Biavati, J. Bidlot, M. Bonavita, G. Chiara, P. Dahlgren, D. Dee, M. Diamantakis, R. Dragani, J. Flemming, R. Forbes, M. Fuentes, A. Geer, L. Haimberger, S. Healy, R. J. Hogan, E. Hólm, M. Janisková, S. Keeley, P. Laloyaux, P. Lopez, C. Lupu, G. Radnoti, P. Rosnay, I. Rozum, F. Vamborg, S. Villaume, J.-N. Thépaut, The ERA5 global reanalysis, Quarterly Journal of the Royal Meteorological Society 146 (730) (2020) 1999–2049. doi:https://doi.org/10.1002/qj.3803.

[44] EIA, Form EIA-860 detailed data with previous form data (EIA-860A/860B), https://www.eia.gov/electricity/data/eia860/ (Sep. 2022).

[45] G. Buster, M. Rossol, P. Pinchuk, R. Spencer, B. N. Benton, M. Bannister, T. Williams, The renewable energy potential model (rev) (Feb. 2023). doi:https://doi.org/10.5281/zenodo.7641483.

[46] M. Sengupta, Y. Xie, A. Lopez, A. Habte, G. Maclaurin, J. Shelby, The national solar radiation data base (NSRDB), Renewable and Sustainable Energy Reviews 89 (2018) 51–60. doi:https://doi.org/10.1016/j.rser.2018.03.003.

[47] A. Campbell, C. Bracken, S. Underwood, N. Voisin, A multi-decadal hourly coincident wind and solar power production dataset for the contiguous us, Submitted (2024).

[48] X. Liang, D. P. Lettenmaier, E. F. Wood, S. J. Burges, A simple hydrologically based model of land surface water and energy fluxes for general circulation models, Journal of Geophysical Research: Atmospheres 99 (D7) (2012) 14415–14428. doi:10.1029/94jd00483.
URL https://agupubs.onlinelibrary.wiley.com/doi/pdfdirect/10.1029/94JD00483?download=true

[49] J. J. Hamman, B. Nijssen, T. J. Bohn, D. R. Gergel, Y. Mao, The variable infiltration capacity model version 5 (vic-5): infrastructure improvements for new applications and reproducibility, Geoscientific Model Development 11 (8) (2018) 3481–3496. doi:10.5194/gmd-11-3481-2018.
URL https://gmd.copernicus.org/articles/11/3481/2018/gmd-11-3481-2018.pdf

[50] Y. Yang, M. Pan, H. E. Beck, C. K. Fisher, R. E. Beighley, S.-C. Kao, Y. Hong, E. F. Wood, In quest of calibration density and consistency in hydrologic modeling: Distributed parameter calibration against streamflow characteristics, Water Resources Research 55 (9) (2019) 7784–7803. doi:https://doi.org/10.1029/2018WR024178.

[51] Y. Yang, M. Pan, P. R. Lin, H. E. Beck, Z. Z. Zeng, D. Yamazaki, C. H. David, H. Lu, K. Yang, Y. Hong, E. F. Wood, Global reach-level 3-hourly river flood reanalysis (1980-2019), Bulletin of the American Meteorological Society 102 (11) (2021) E2086–E2105, zc1gv Times Cited:25 Cited References Count:100. doi:10.1175/Bams-D-20-0057.1.
URL <GotoISI>://WOS:000757278200004

[52] T. Thurber, C. Vernon, N. Sun, S. Turner, J. Yoon, N. Voisin, mosartwmpy: A python implementation of the mosart-wm coupled hydrologic routing and water management model, Journal of Open Source Software 6 (62) (2021). doi:10.21105/joss.03221.
URL https://joss.theoj.org/papers/10.21105/joss.03221.pdf

[53] H. Y. Li, M. S. Wigmosta, H. Wu, M. Y. Huang, Y. H. Ke, A. M. Coleman, L. R. Leung, A physically based runoff routing model for land

surface and earth system models, Journal of Hydrometeorology 14 (3) (2013) 808–828, 162xz Times Cited:158 Cited References Count:61. doi:10.1175/Jhm-D-12-015.1.

[54] N. Voisin, H. Li, D. Ward, M. Huang, M. Wigmosta, L. R. Leung, On an improved sub-regional water resources management representation for integration into earth system models, Hydrology and Earth System Sciences 17 (9) (2013) 3605–3622. doi:10.5194/hess-17-3605-2013. URL https://hess.copernicus.org/articles/17/3605/2013/hess-17-3605-2013.pdf

[55] S. W. D. Turner, J. C. Steyaert, L. Condon, N. Voisin, Water storage and release policies for all large reservoirs of conterminous united states, Journal of Hydrology 603 (2021). doi:10.1016/j.jhydrol.2021.126843.

[56] D. Broman, N. Voisin, S.-C. Kao, A. Fernandez, G. R. Ghimire, Multi-scale impacts of climate change on hydropower for long-term water-energy planning in the contiguous united states, Environmental Research Letters 19 (9) (2024) 094057. doi:https://doi.org/10.1088/1748-9326/ad6ceb.

[57] S. W. D. Turner, N. Voisin, J. Fazio, D. Hua, M. Jourabchi, Compound climate events transform electrical power shortfall risk in the pacific northwest, Nat Commun 10 (1) (2019) 8, turner, S W D Voisin, N Fazio, J Hua, D Jourabchi, M eng Research Support, Non-U.S. Gov't Research Support, U.S. Gov't, Non-P.H.S. England 2019/01/04 Nat Commun. 2019 Jan 2;10(1):8. doi: 10.1038/s41467-018-07894-4. doi:10.1038/s41467-018-07894-4. URL https://www.ncbi.nlm.nih.gov/pubmed/30602781https://www.ncbi.nlm.nih.gov/pmc/articles/PMC6315041/pdf/41467_2018_Article_7894.pdf

[58] K. Doering, C. L. Anderson, S. Steinschneider, Evaluating the intensity, duration and frequency of flexible energy resources needed in a zero-emission, hydropower reliant power system, Oxford Open Energy 2 (2023). doi:https://doi.org/10.1093/ooenergy/oiad003.

[59] Grid Deployment Office, The nationaltransmission planning study, Tech. rep., U.S. Department of Energy, Grid Deployment Office.

2024. The NationalTransmission Planning Study. Washington, D.C.: U.S. Department of Energy.https://www.energy.gov/gdo/national-transmission-planning-study., Washington, D.C. (2024). URL https://www.energy.gov/gdo/national-transmission-planning-study

[60] F. Mockert, C. M. Grams, T. Brown, F. Neumann, Meteorological conditions during periods of low wind speed and insolation in germany: The role of weather regimes, Meteorological Applications 30 (4) (Jul. 2023). doi:https://doi.org/10.1002/met.2141.

[61] H. Hersbach, B. Bell, P. Berrisford, G. Biavati, A. Horányi, J. Muñoz Sabater, J. Nicolas, C. Peubey, R. Radu, I. Rozum, D. Schepers, A. Simmons, C. Soci, D. Dee, J.-N. Thépaut, Era5 hourly data on single levels from 1940 to present, Copernicus Climate Change Service (C3S) Climate Data Store (CDS) (2023). doi:https://doi.org/10.24381/cds.adbb2d47.

[62] Y. Ou, G. Iyer, H. McJeon, R. Cui, A. Zhao, K. T. O'Keefe, M. Zhao, Y. Qiu, D. H. Loughlin, State-by-state energy-water-land-health impacts of the us net-zero emissions goal, Energy and Climate Change 4 (2023) 100117. doi:https://doi.org/10.1016/j.egycc.2023.100117.

[63] Y. Ou, Y. Zhang, S. Waldhoff, G. Iyer, Gcam-usa scenarios for godeeep (2024). doi:https://doi.org/10.5281/ZENODO.10642507.

[64] D. Yates, J. K. Szinai, A. D. Jones, Modeling the water systems of the western us to support climate-resilient electricity system planning, Earth's Future 12 (1) (Dec. 2023). doi:https://doi.org/10.1029/2022EF003220.

Supplemental material for Seasonal compound renewable energy droughts in the Unites States

---

The investigation into the weather mechanisms driving the occurrence of seasonal energy droughts across various regions highlights important atmospheric variables influencing energy resources. In the Pacific Northwest (PNW: PSEI, BPAT, PGE, and PACW) cluster, strong negative anomalies of 850 hPa's relative humidity (RH-850 in Figure S2) and upwind dry conditions (WindSH-850 in Figure S2) typically influence solar energy. However, as solar is not a dominant energy source in the PNW, these results are misleading. On the other hand, strong negative anomalies in Wind10 due to a typical Arctic Ridge pattern (GPH-500 in Figure S2) indicate a decrease in wind speed. Integrated water vapor (IWV in Figure S2) shows moderate negative anomalies, indicating reduced atmospheric moisture, while vapor pressure deficit (VPD in Figure S2) has moderate positive anomalies, signaling increased drying potential.

Similar to PNW, RH-850 and WindSH-850 conditions cannot explain the solar droughts for the California (CA: CISO and LDWP) cluster. For this cluster, wind speed, IWV, and VPD assist both wind and hydro energy droughts except that the low wind condition is induced by a Pacific Trough pattern instead of an Arctic Ridge, as seen in the PNW.

For the Intermountain West (NWMT, PACE, WACM, and PSCO) and Inner West (AVA, IPCO, NEVP, WALC, and SRP) clusters, strong positive anomalies in RH850 indicate excessive cloud cover, whereas moderate negative anomalies in Wind10 and an Arctic High pattern (GPH-500) suggest reduced wind speeds, thus favoring wind energy droughts. Again, minimal signals in IWV and VPD anomalies shown over the region can hardly explain the causes of the hydro energy droughts.

The Midwest cluster, including SWPP, SPA, AECI, ERCO, and MISO, displays strong positive RH850 anomalies and typical negative Wind10 anomalies associated with an Arctic High pattern (GPH500). This indicates similar effects with notable cloud cover reducing solar energy and diminished wind

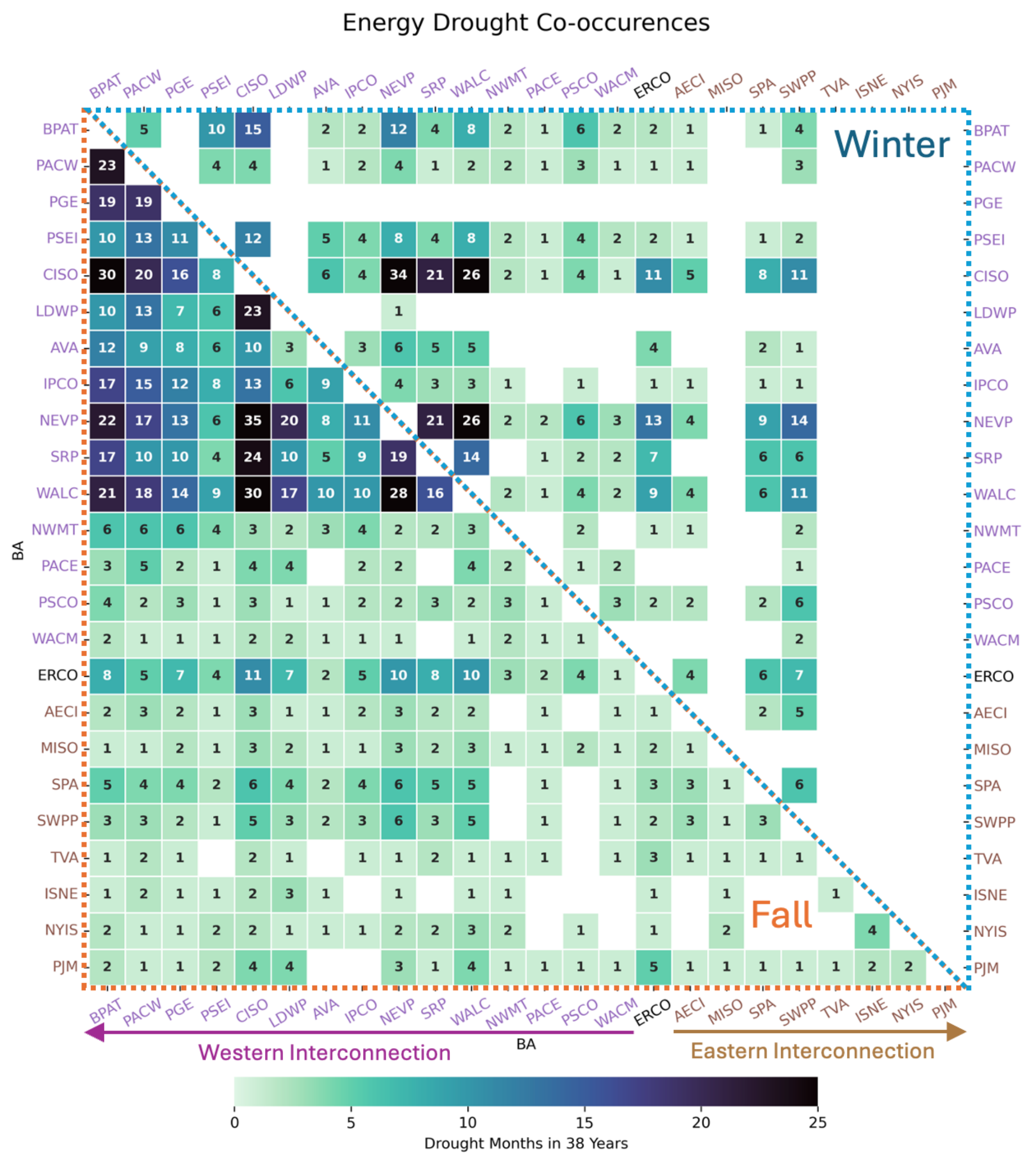

Figure S1: Co-occurrence heat map of compound VRE droughts. The element values indicate the number of months in which compound VRE droughts co-occur between two BAs within the 114 months for each season over 1982-2019, which corresponds to the spatial networks illustrated in Figure 3a in the paper. The lower triangular section represents data from fall, while the upper triangular section represents data from winter. The BAs are sorted by NERC grid interconnection and Cluster in Table 1.

speeds affecting wind energy availability. However, both IWV and VPD show favorable hydro energy sources for the top 4 compound drought months, which is as puzzling as the TVA hydro situation described below.

In the Northeast cluster (NE: PJM, NYIS, and ISNE), moderate positive anomalies in 850 hPa relative humidity (RH850) signify enhanced cloud cover contributing to solar energy droughts, along with moderate negative anomalies in 10-meter wind (Wind10) indicating increased wind energy droughts. The 500 hPa Geopotential height (GPH500) shows positive anomalies centered on the Northeast offshore, forming a moderate Pacific Trough pattern, which is associated with a negative wind anomaly over the U.S. Northeast. Integrated Water Vapor (IWV) also shows moderate negative anomalies, suggesting reduced atmospheric moisture, while Vapor Pressure Deficit (VPD) has moderate positive anomalies, implying a higher drying potential, and enhancing hydro energy droughts.

Lastly, the TVA cluster (TVA) experiences strong positive RH-850 anomalies, signaling significant cloud cover. Interestingly, IWV and VPD show favorable hydroenergy conditions. Further investigation reveals that hydro dominates the drought event for only one month out of the top four drought months. However, three energy sources combined become compound energy droughts, indicating the complexity of drought characteristics between single energy sources and compound energy forms. Additionally, composite Wind10 or GPH500 has no clear indication for wind energy droughts due to limited wind energy infrastructure in this region; hydro and solar are the primary renewable energy sources.

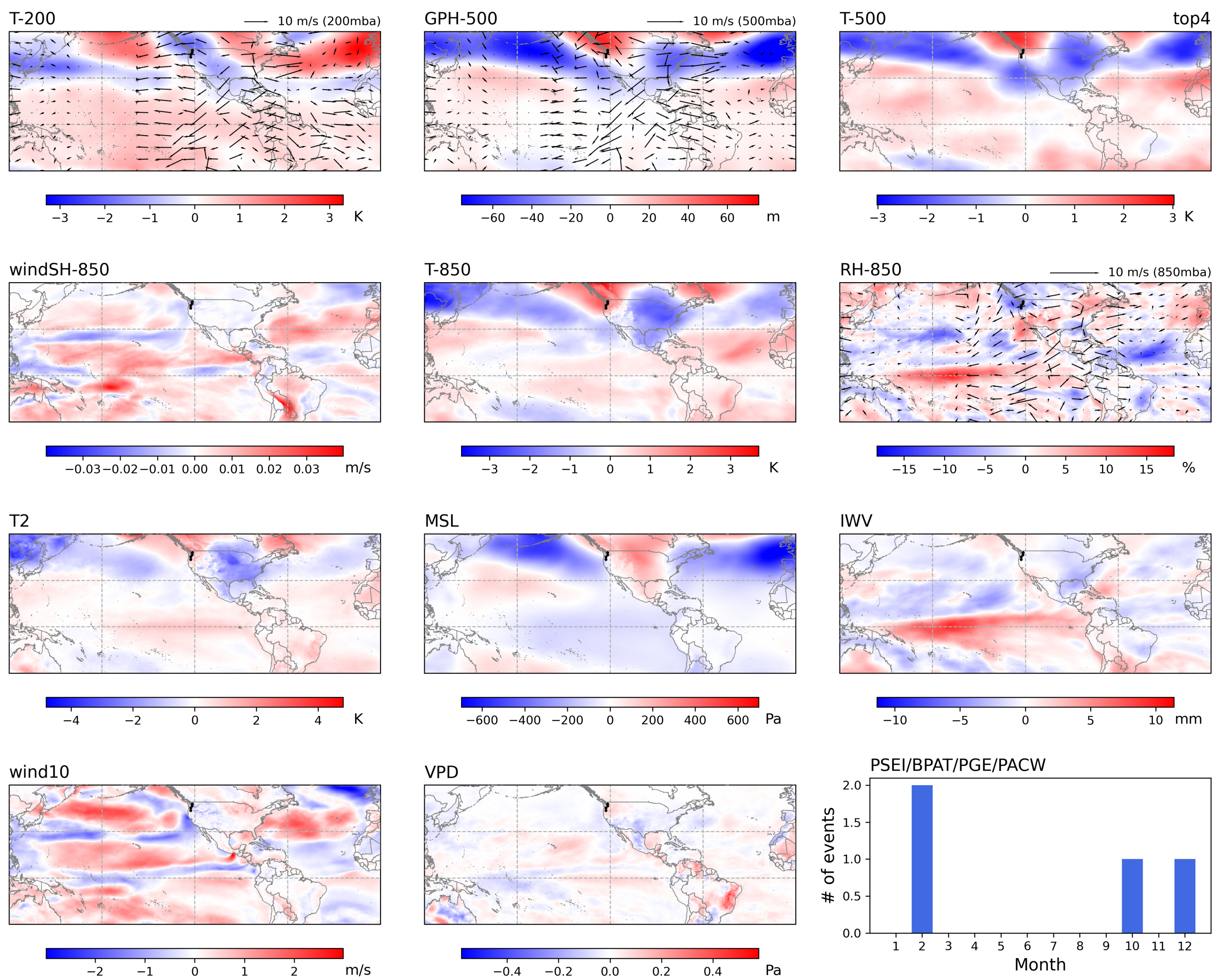

Figure S2: Composite monthly anomalies of Top 4 compound energy droughts for Pacific Northwest. The scale circulation fields include 200 hPa's temperature (T-200), 500 hPa's Geopotential height (GPH-500) and temperature (T-500), 850 hPa's moisture transport (windSH-850), temperature (T-850), and relative humidly (RH-850), 2 meter temperature (T2), mean sea level pressure (MSL), integrated water vapor (IWV), 10 meter's wind (wind10), and vapor pressure deficit (VPD). Arrows in the figures denote the wind vectors at the given level. Bar chat indicates the months the Top 4 events appear.

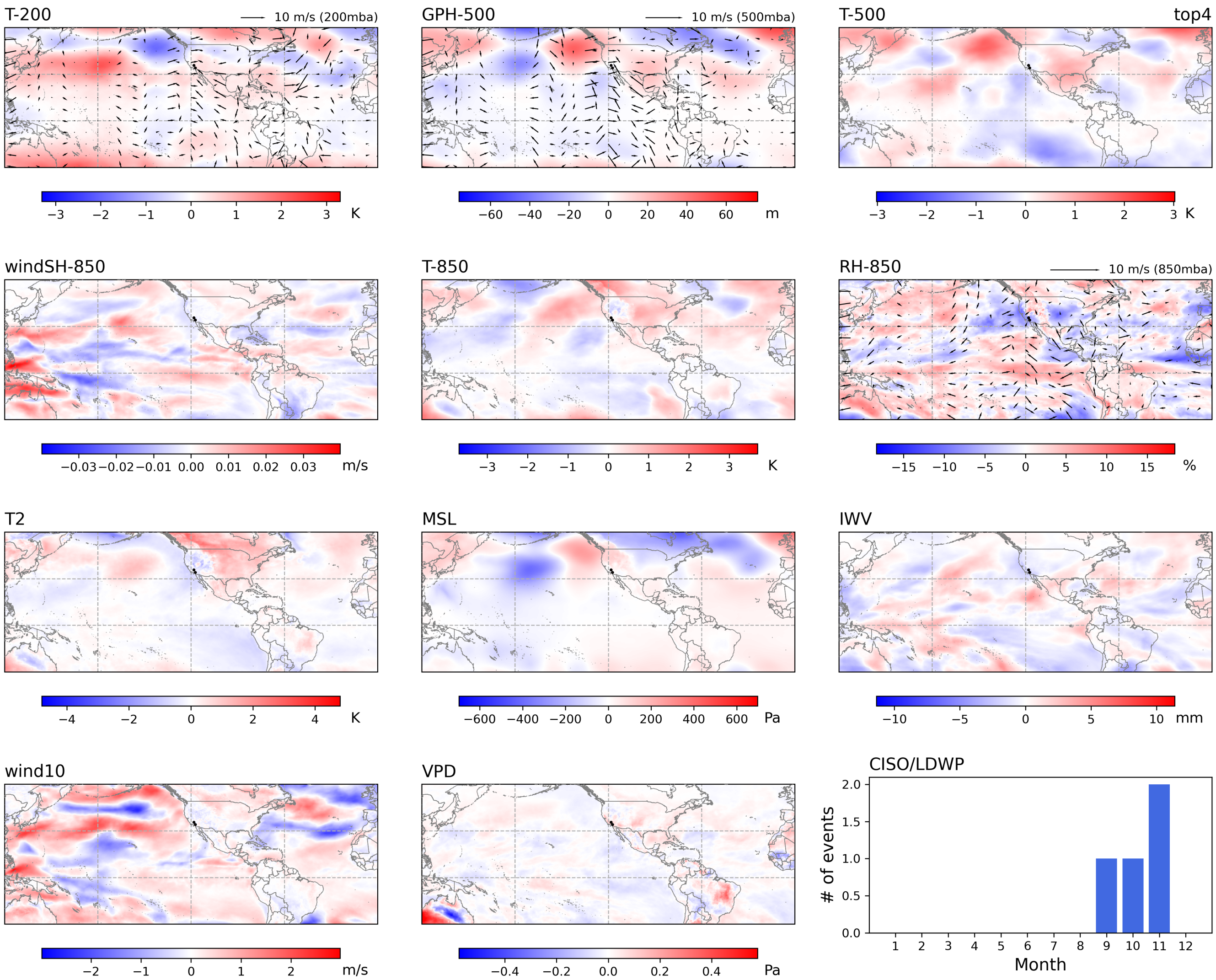

Figure S3: Same as S2 but for CA

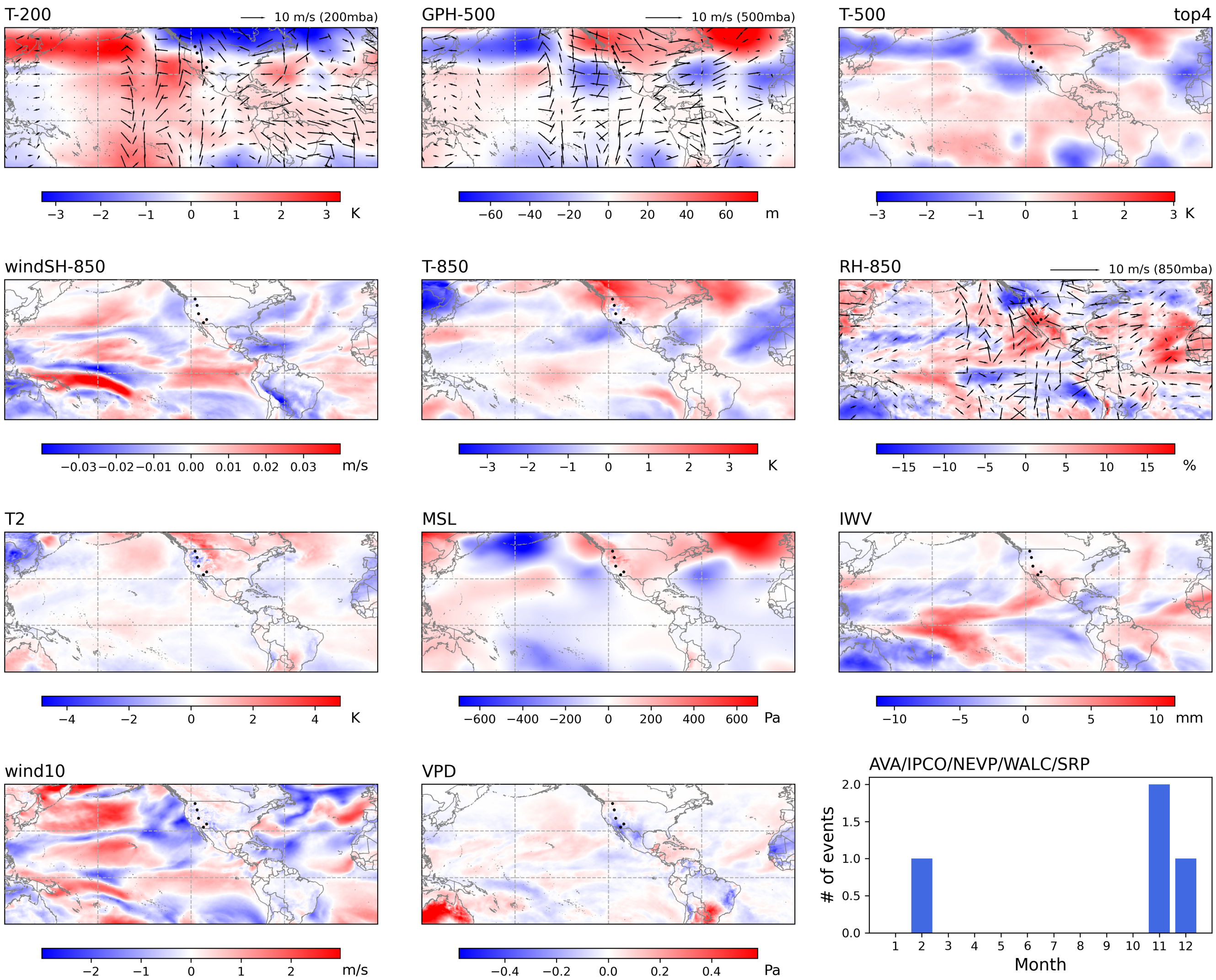

Figure S4: Same as S2 but for Inner West

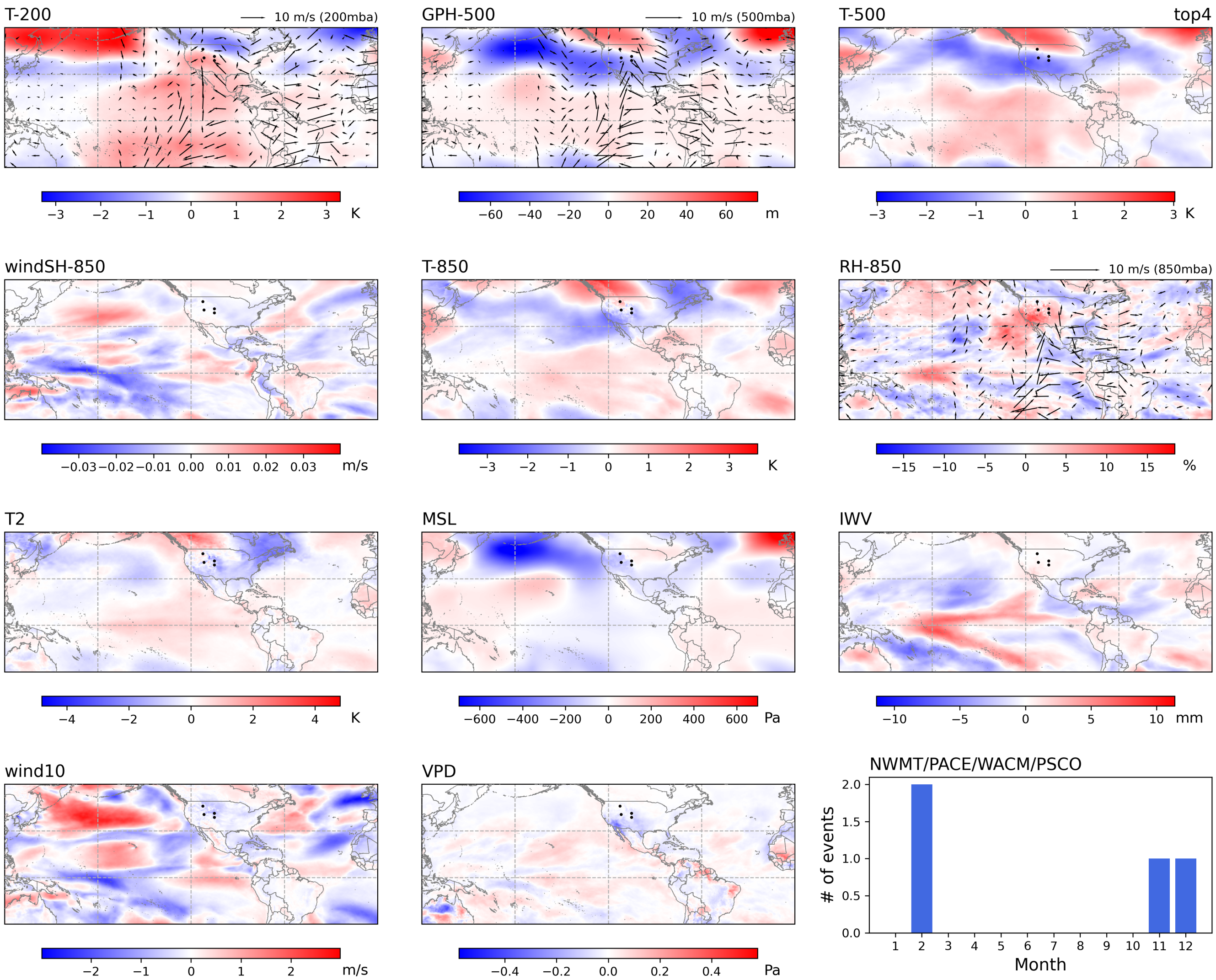

Figure S5: Same as S2 but for Intermountain West

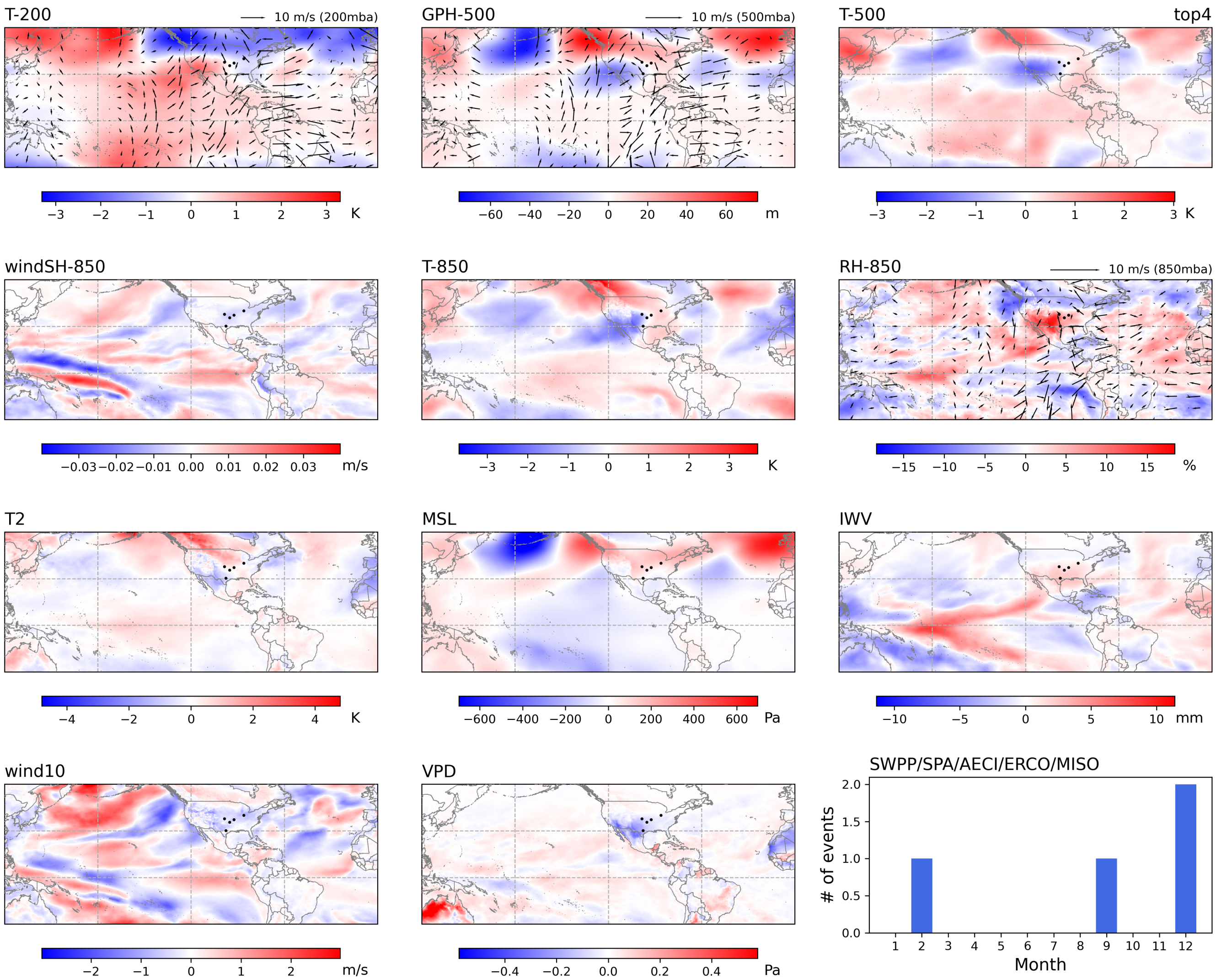

Figure S6: Same as S2 but for Midwest

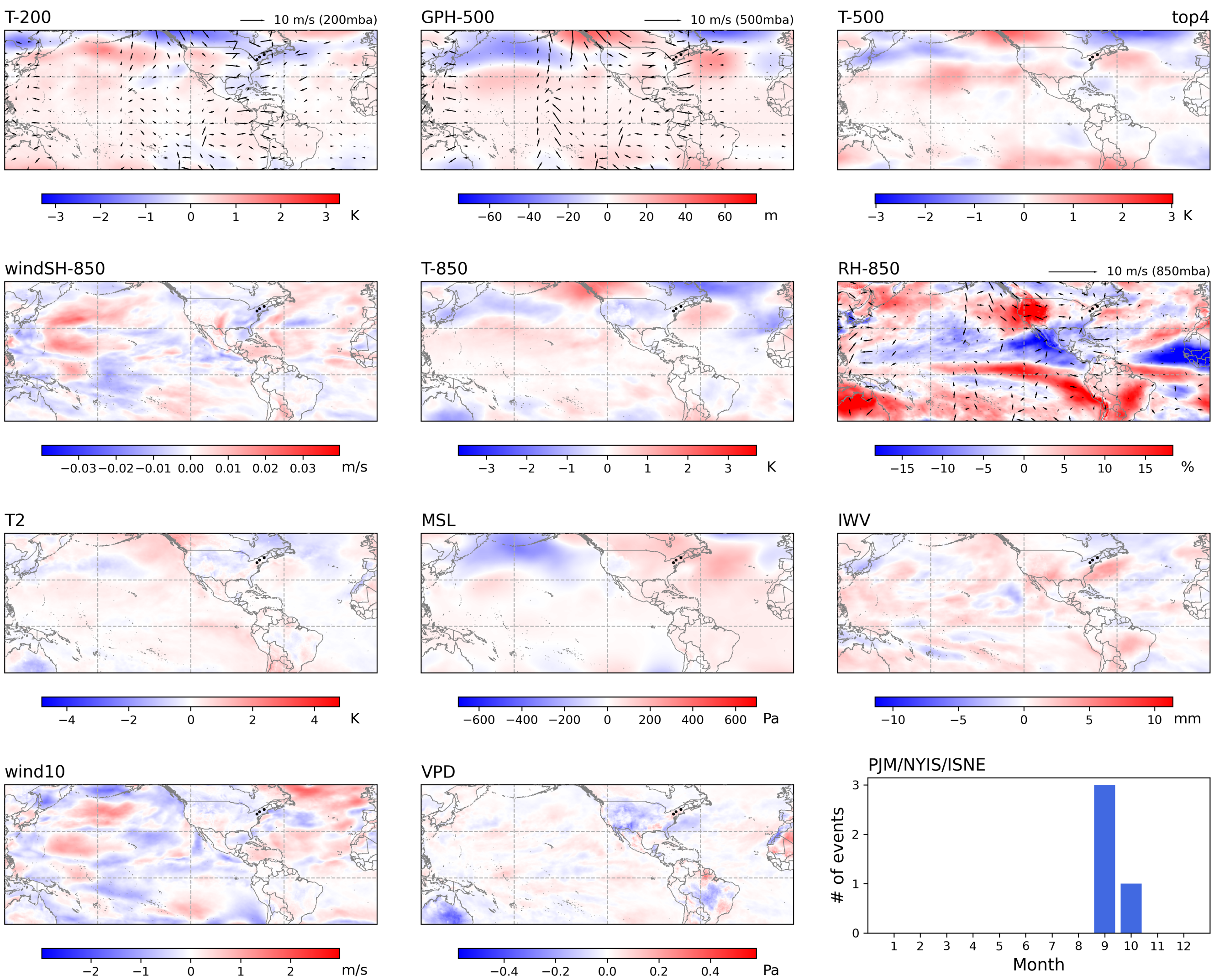

Figure S7: Same as S2 but for Northeast

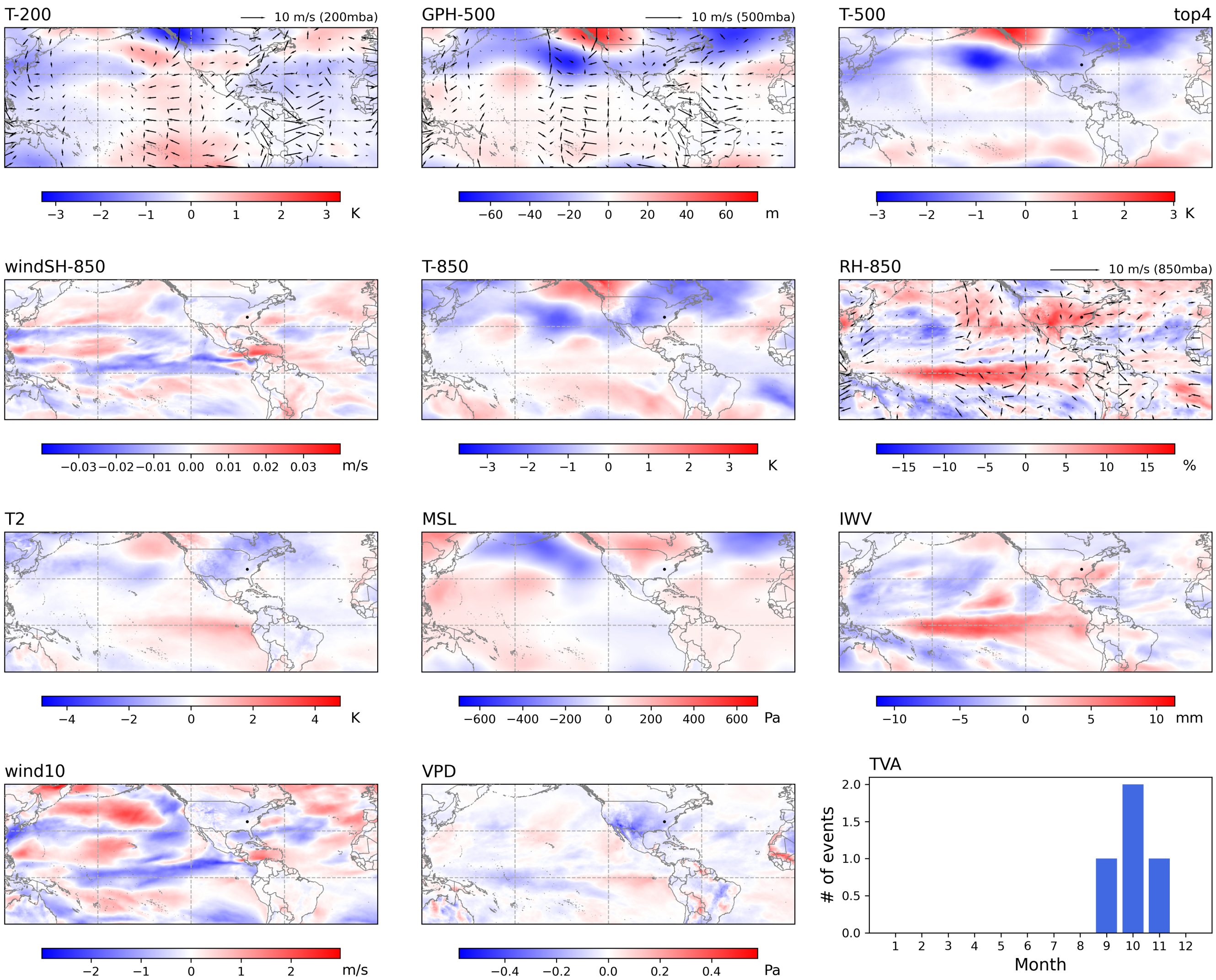

Figure S8: Same as S2 but for TVA

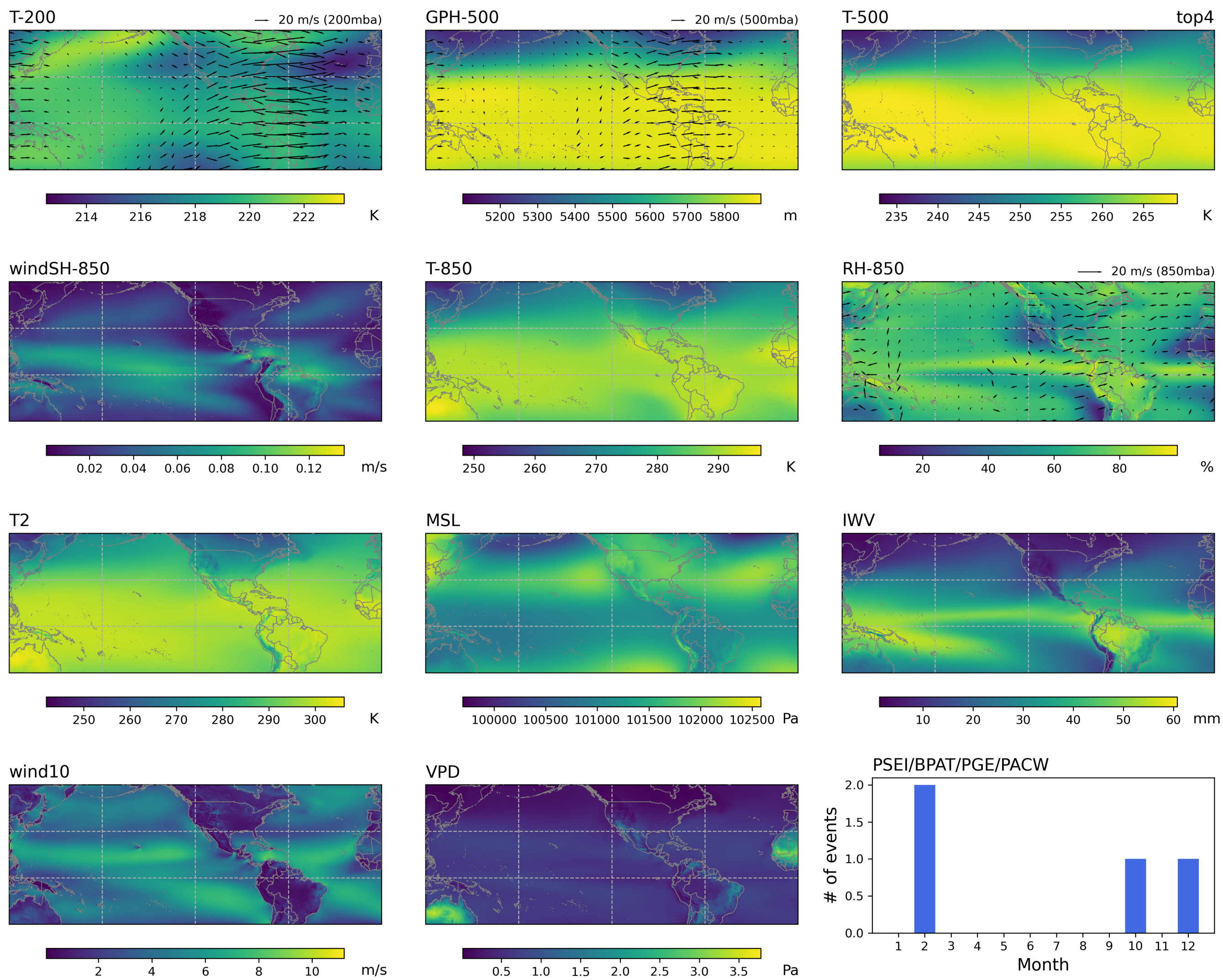

Figure S9: Climatology of the large scale circulation fields for the top 4 compound drought events for the Pacific Northwest, including 200 hPa's temperature (T-200), 500 hPa's Geopotential height (GPH-500) and temperature (T-500), 850 hPa's moisture transport (windSH-850), temperature (T-850), and relative humidly (RH-850), 2 meter temperature (T2), mean sea level pressure (MSL), integrated water vapor (IWV), 10 meter's wind (wind10), and vapor pressure deficit (VPD). Arrows denote the wind vectors at the given level.

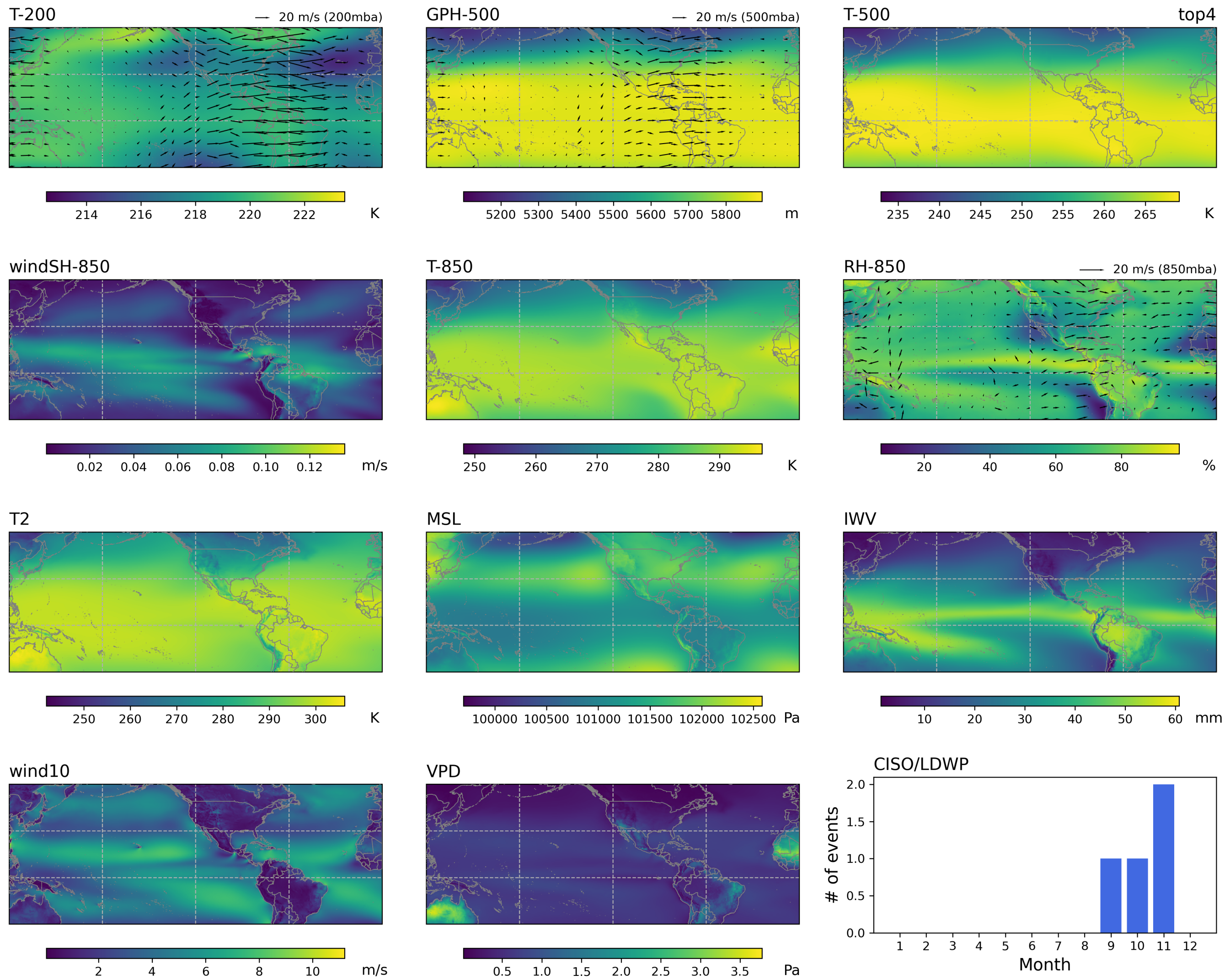

Figure S10: Same as S9 but for CA

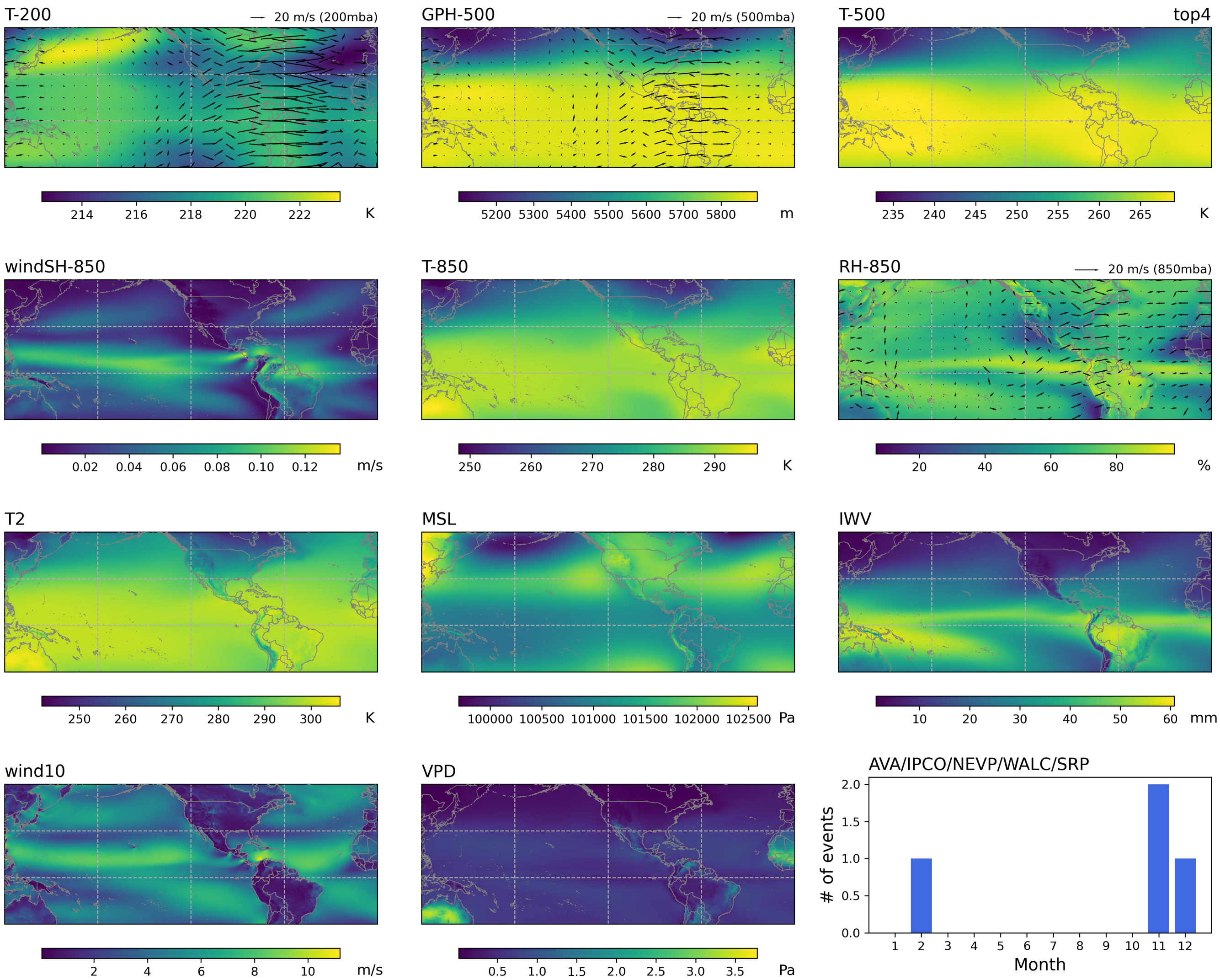

Figure S11: Same as S9 but for Inner West

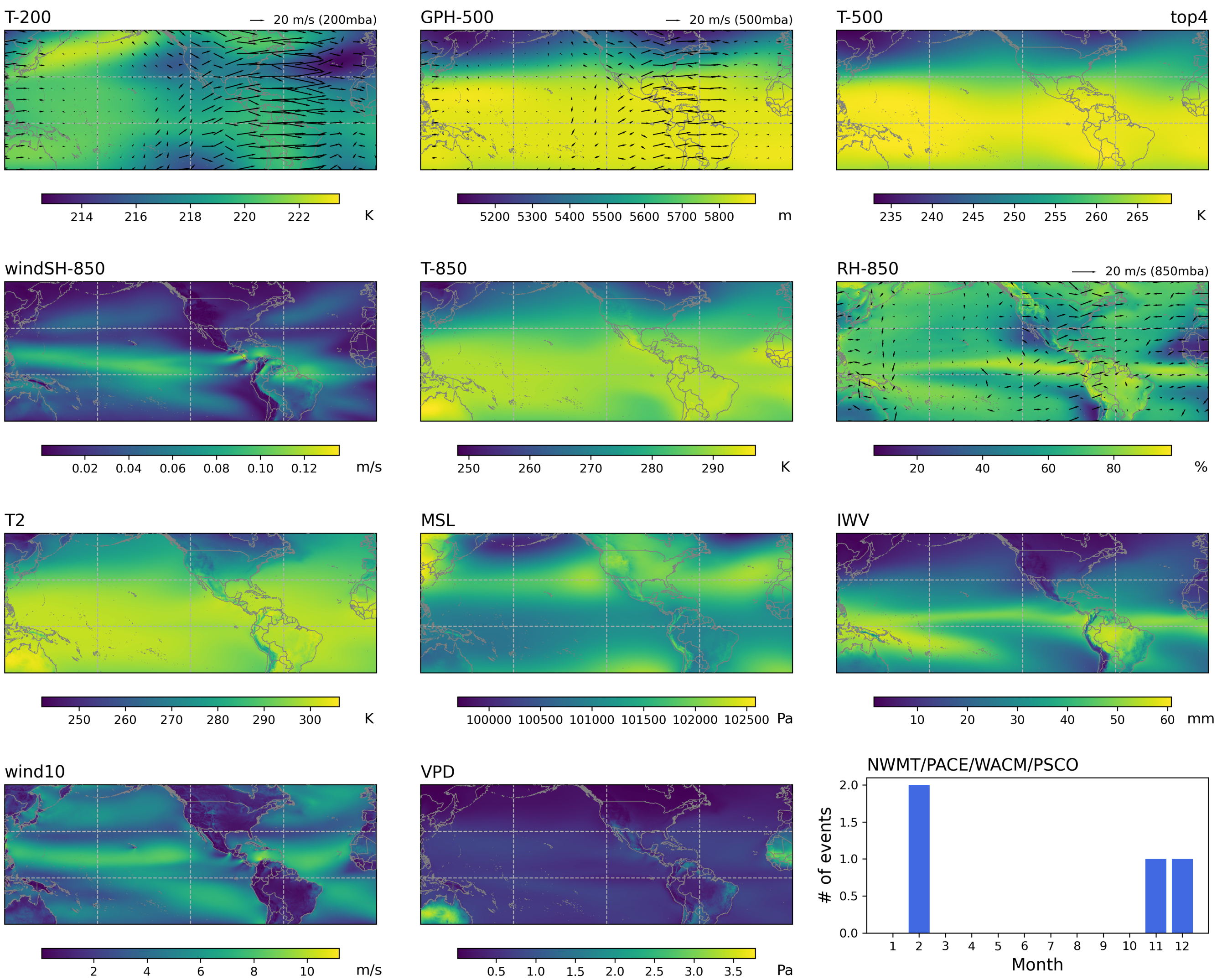

Figure S12: Same as S9 but for Intermountain West

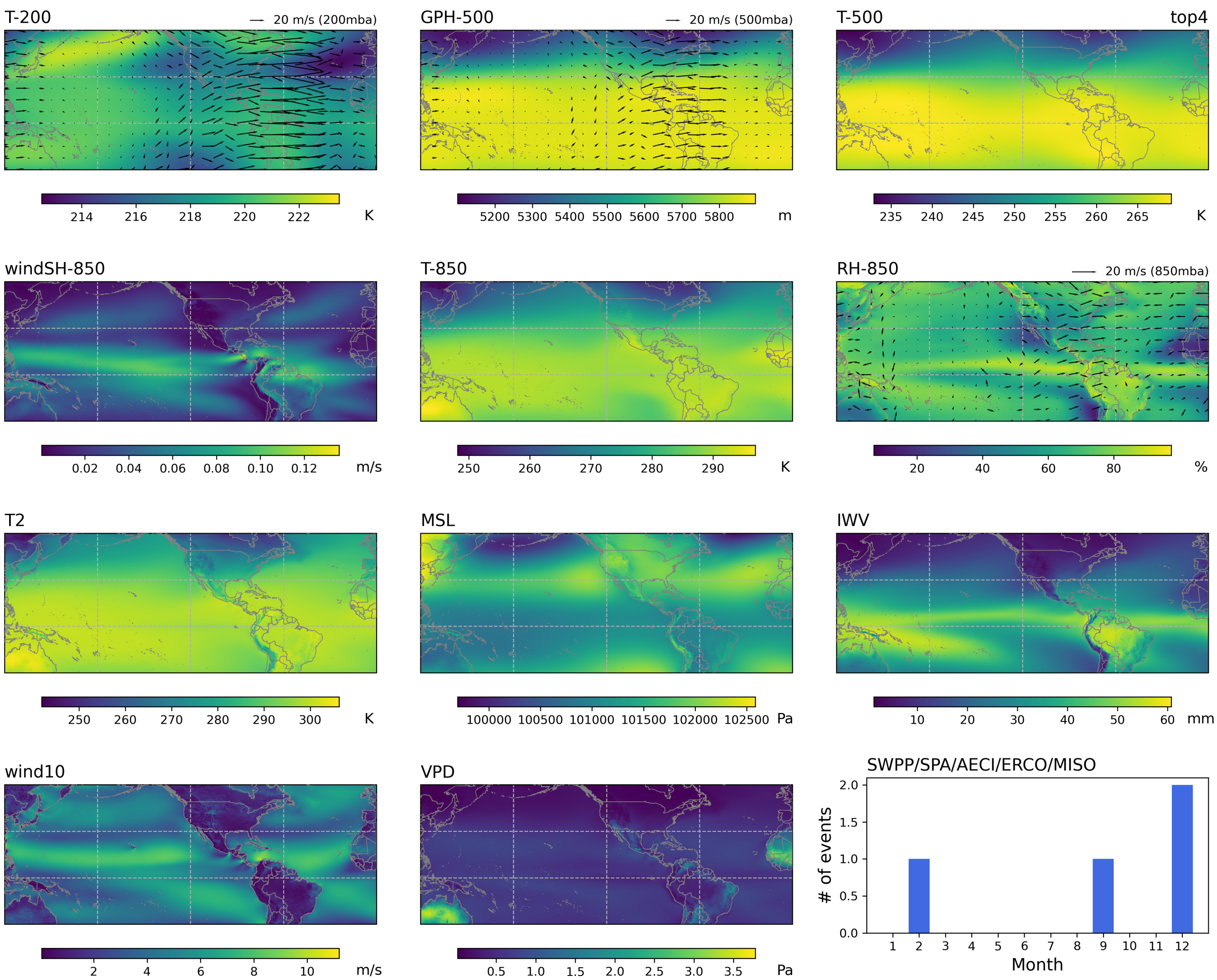

Figure S13: Same as S9 but for Midwest

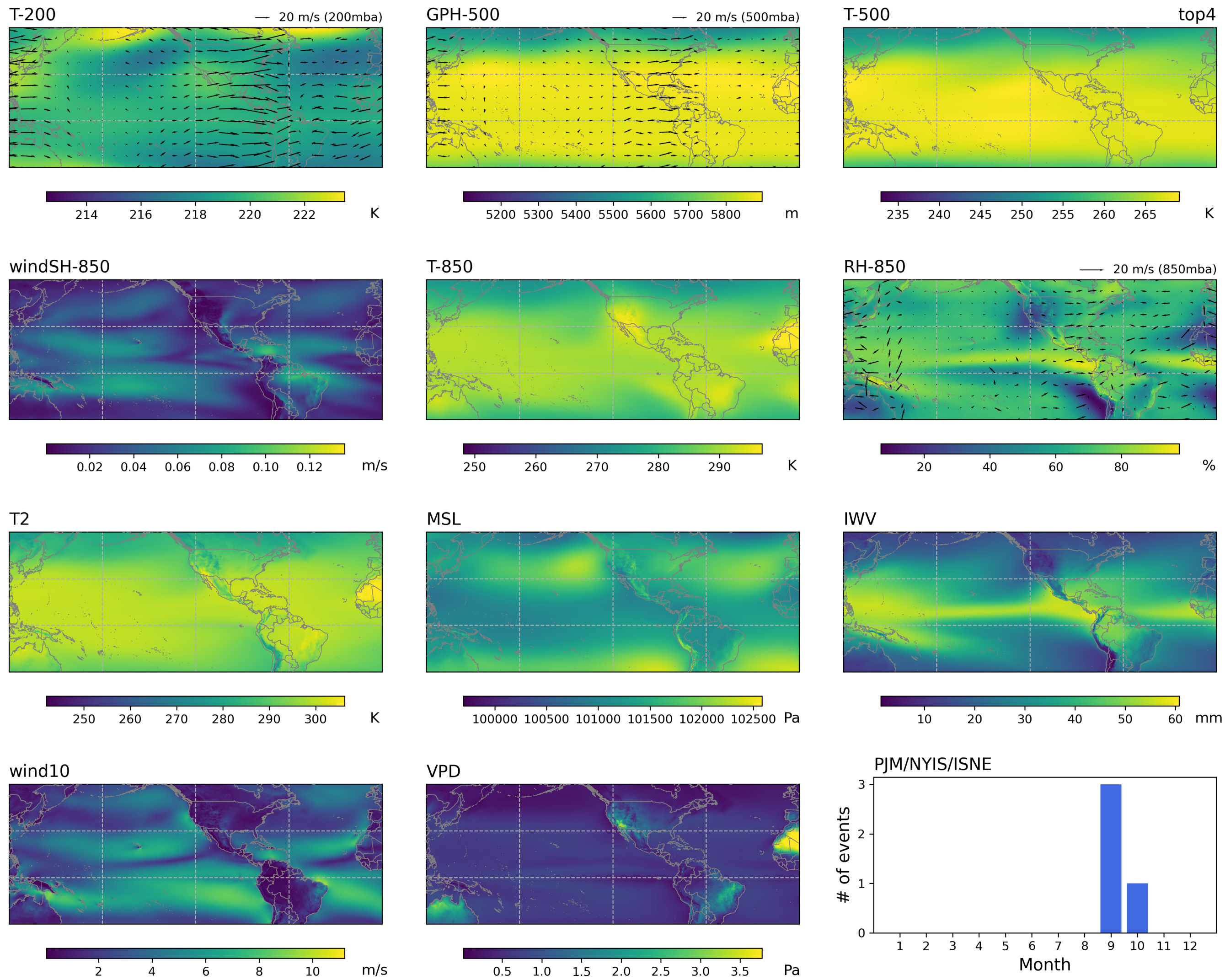

Figure S14: Same as S9 but for Northeast

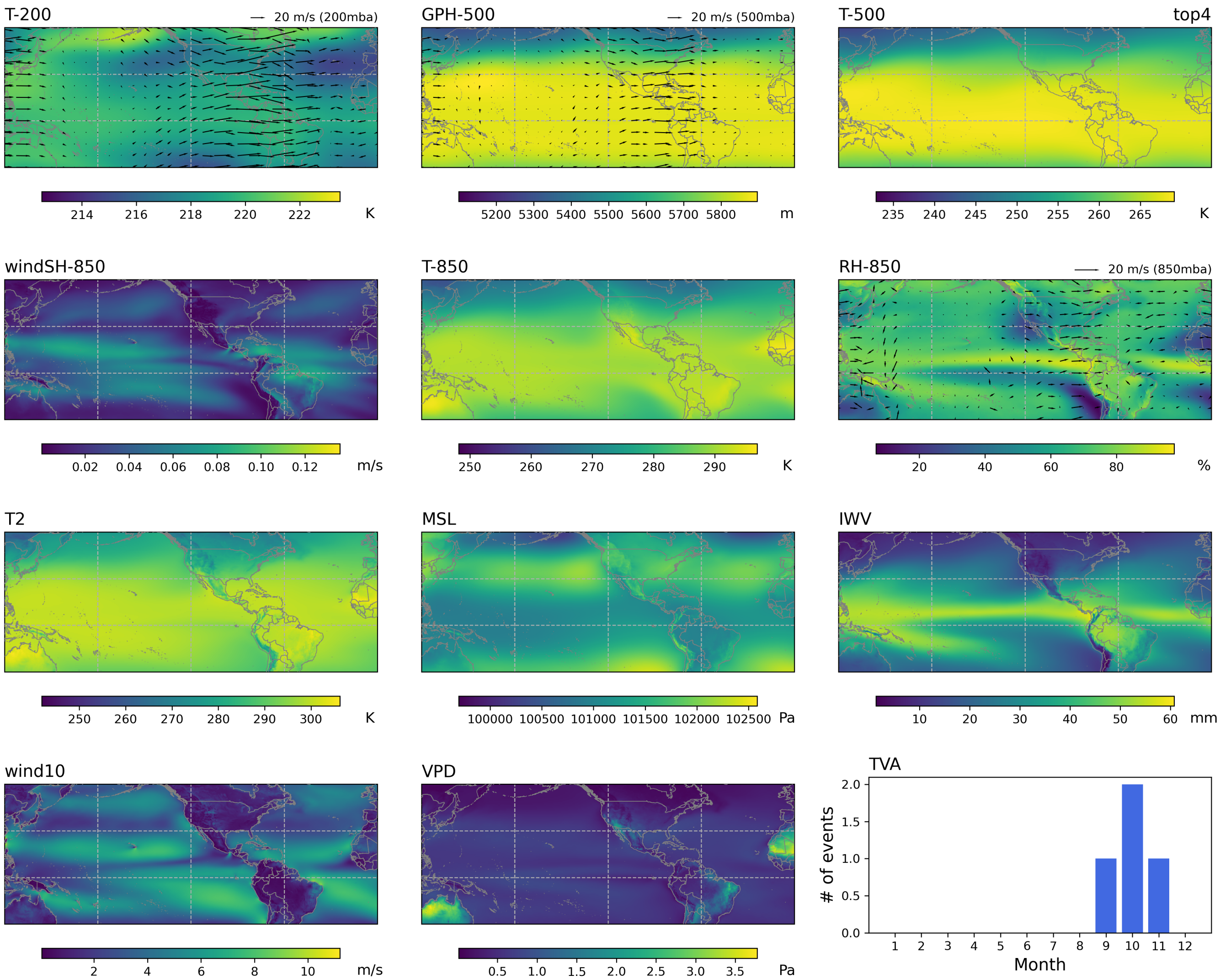

Figure S15: Same as S9 but for TVA